Supramolecular Chemistry
Publication details, including instructions for authors and subscription information:
http://www.informaworld.com/smpp/title~content=t713649759

Strong Positive Allosterism which Appears in Molecular Recognition with Cerium(IV) Double Decker Porphyrins: Correlation between the Number of Binding Sites and Hill Coefficients

Masato Ikeda[a]; Masayuki Takeuchi[a]; Atsushi Sugasaki[a]; Andrew Robertson[a]; Tomoyuki Imada[a]; Seiji Shinkai[a]
[a] Department of Chemistry & Biochemisry, Graduate School of Engineering, Kyushu University, Fukuoka, Japan

To cite this Article Ikeda, Masato , Takeuchi, Masayuki , Sugasaki, Atsushi , Robertson, Andrew , Imada, Tomoyuki and Shinkai, Seiji(2000) 'Strong Positive Allosterism which Appears in Molecular Recognition with Cerium(IV) Double Decker Porphyrins: Correlation between the Number of Binding Sites and Hill Coefficients', Supramolecular Chemistry, 12: 3, 321 — 345
To link to this Article: DOI: 10.1080/10610270008029453
URL: http://dx.doi.org/10.1080/10610270008029453

SUPRAMOLECULAR CHEMISTRY, Vol. 12, pp. 321-345
Reprints available directly from the publisher
Photocopying permitted by license only

Strong Positive Allosterism which Appears in Molecular Recognition with Cerium(IV) Double Decker Porphyrins: Correlation between the Number of Binding Sites and Hill Coefficients

MASATO IKEDA, MASAYUKI TAKEUCHI, ATSUSHI SUGASAKI, ANDREW ROBERTSON, TOMOYUKI IMADA and SEIJI SHINKAI*

Department of Chemistry & Biochemisry, Graduate School of Engineering, Kyushu University, Fukuoka 812–8581, Japan

(Received April 10, 2000; In final form May 02, 2000.)

Cerium(IV) double decker porphyrins bearing one-to-four pairs of 4-pyridyl groups (3a, 3a', 3bp, 3bd, 3c, and 3d) were synthesized from tetraarylporphyrins bearing mono-, bis-, tris-, and tetrakis(4-pyridyl) groups. In 3b bearing two pairs of 4-pyridyl groups, there exist two isomers in which the 4-pyridyl groups are either proximal or distal (3bp and 3bd, respectively). In a mixed solvent of dichloromethane: ethyl acetate (30:1 v/v), 3a' bearing one pair of 4-pyridyl groups and three pairs of phenyl groups did not interact with any dicarboxylic acids whereas 3d bearing four pairs of 4-pyridyl groups interacted only with dicarboxylic acid guests with a dimethylene spacer [e.g., BOC-L-aspartic acid (L-4) and (1R,2R)-cyclohexane-1,2-dicarboxylic acid ((1R,2R)-5)]. Interestingly, the complexation process monitored by CD spectroscopy showed a positive homotropic allosterism which satisfied the Hill equation giving constants $K = 2.63 \times 1011M^{-4}$ and $n = 3.9$ for L-4 and $K = 2.75 \times 109\ M^{-4}$ and $n = 4.0$ for (1R,2R)-5. The continuous variation plots (Job plots) also supported the formation of the 1:4 3d/dicarboxylic acid guest complexes. The results consistently indicate that four pairs of 4-pyridyl groups in 3d allosterically bind these guests. In 3d, the two porphyrin rings can still rotate, but once the rotation is suppressed by the first guest binding, the subsequent binding of the second, third and fourth guests can occur cooperatively. This is the origin of the present positive homotoropic allosterism. A similar positive homotropic allosterism was also observed for 3bp and 3bd with $n = 1.5$ and 1.7, respectively and 3c with $n = 3.0$. The X-ray crystallographic study of the 3d·[(1R,2R)-5]4 complex showed that the two porphyrin planes are warped outward to relax the electrostatic repulsion and chirally twisted. The two carboxylic acid groups form intermolecular hydrogen bonds (but not intramolecular bridge-type hydrogen bonds) with the pyridyl groups because of the close packing effect of rigid host 3d and rigid guest (1R,2R)-5. In conclusion, this is a rare example of positive homotropic allosterism in an artificial system which is frequently seen in nature where the biological events must be efficiently regulated in response to signals.

Keywords: Double decker porphyrins, positive allosterism, molecular recognition, chirality, crystal structure

INTRODUCTION

Positive or negative allosterisms are ubiquitously seen in nature where the biological events must be efficiently regulated in response to chemical or physical signals from the outside world. The typical examples are observed for a

* Corresponding Author.

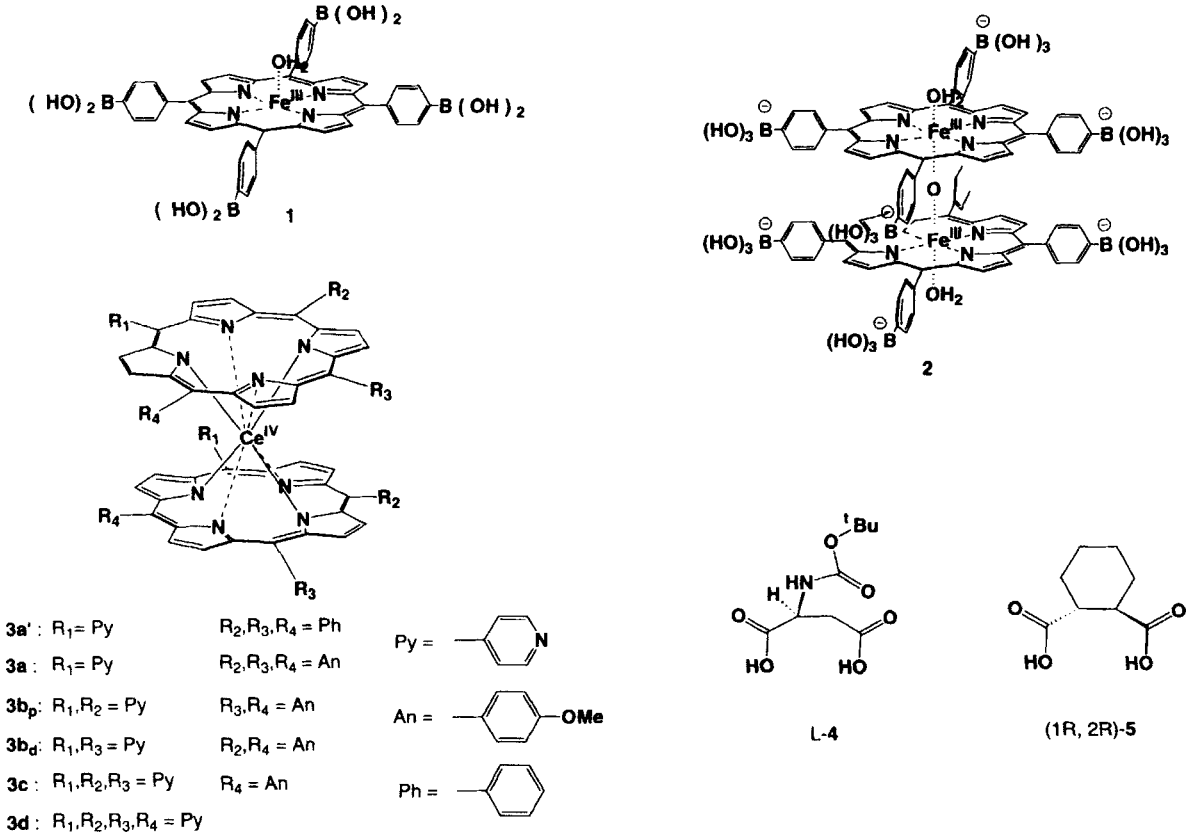

SCHEME 1

cooperative dioxygen binding to hemoglobin,[1] hexamerization of arginine repressor,[2] a cooperative effect with respect to the concentration of arachidonate-containing phospholipids in cytosolic phospholipase A_2,[3] *etc.*[4] The biomimetic design of such allosteric systems is of great significance in order to regulate the complexation ability or the catalytic activity of artificial receptors according to an allosteric manner.[6–14] Furthermore, the methodology is very useful to amplify and convert weak chemical or physical signals into other signals which are convenient for us to read out and record. Allosteric systems are classified into four different categories: positive heterotropic, negative heterotropic, positive homotropic, and negative homotropic. There are several examples which successfully reproduce the heterotropic allosteric systems,[6–12] whilst design of homotropic allosteric systems is more difficult but more important for the efficient regulation of equilibria, catalyses, and information transduction.[13,14] To the best of our knowledge, however, there is only one precedent for a positive homotropic system with a large Hill coefficient (n); this system features cooperative binding of saccharides to a resorcinol cyclic tetramer host ($n = 4$).[13a] We have previously synthesized a porphyrinatoiron(III) (**1**) bearing four boronic acid groups.[14] The μ-oxo dimer (**2**), self-assembled at alkaline pH, showed extraordinarily high affinity and selectivity for glucose and galactose, but only one pair of boronic acids was used to form 1:1 complexes with saccharides and residual three pairs of boronic acids were totally inactive for a saccharide-binding.[14] The strong negative homotropic allosterism was

attributed to inclination of two porphyrin planes which was induced by the binding of the first saccharide guest. Here, it occurred to us that if the first guest could suppress the rotation of two porphyrin planes without inclination, the second guest should be bound more efficiently: that is, a positive homotropic allosterism should appear in such a system. To design a porphyrin-based positive homotropic allosteric system we chose a member of cerium(IV) bis(porphyrinate) double deckers[15,16] namely the mono-, di, tri, and tetra(4-pyridyl)porphyrin derivatives (**3a**, $\mathbf{3b_p}$ and $\mathbf{3b_d}$, **3c**, and **3d**, respectively: "p" or "d" denote that the meso-substituents are either proximal or distal: see Scheme 1). These molecules exactly satisfy our requirements: that is, (1) a slow rotation of the two porphyrin planes may be allowed at room temperature, in analogy to similar cerium(IV) bis(diaryl- or bis(tetraaryl-porphyrinates) studied by Aida *et al.*,[16,17] (2) the inclination of two porphyrin planes is more difficult than that of **2**, and (3) 2~4 pairs of 4-pyridyl groups should act as allosteric hydrogen-bonding acceptor sites for diols, hydroxycarboxylic acids, and dicarboxylic acids. Compound **3a** and **3a'** with one pair of pyridyl groups were used as reference compounds. Interestingly, we have found that $\mathbf{3b_p}$, $\mathbf{3b_d}$, **3c**, and **3d** have a sharp positive allosterism, showing high selectivity for certain chiral dicarboxylic acids.[18]

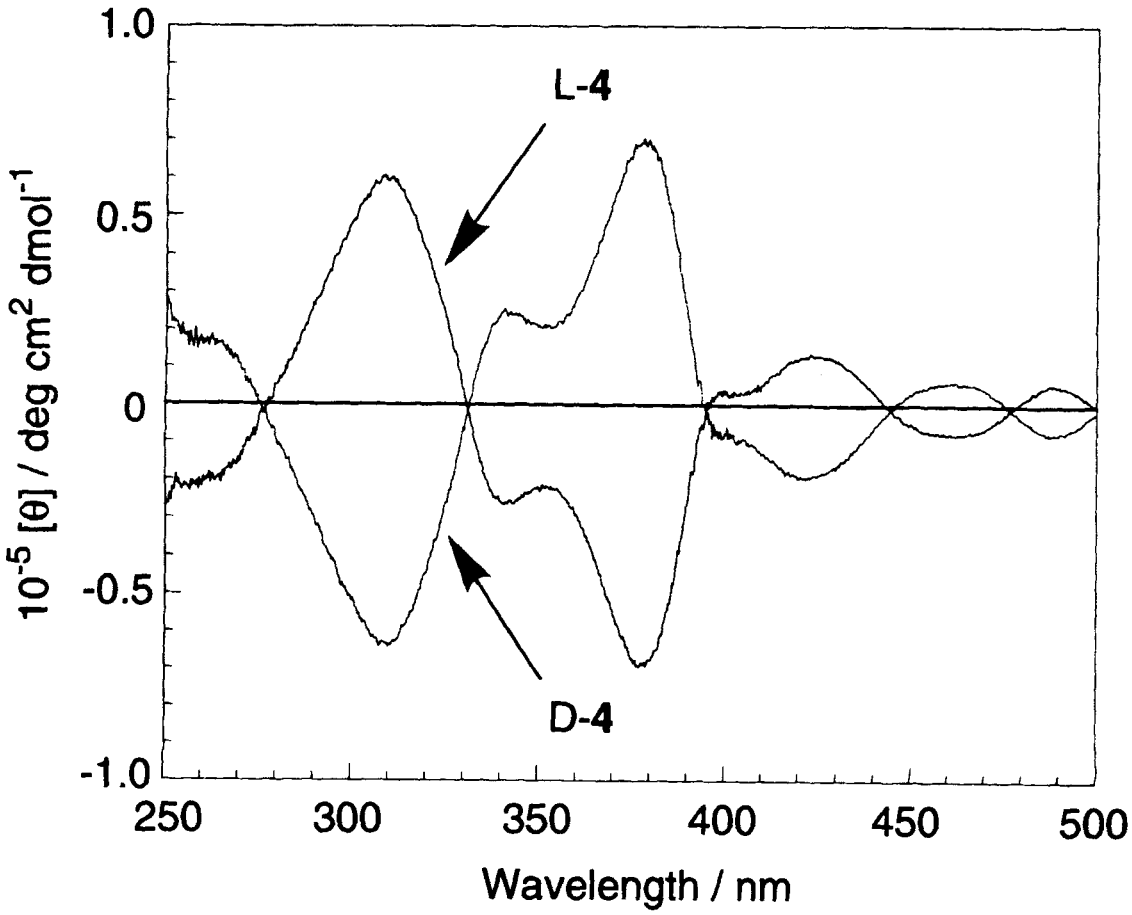

FIGURE 1 CD spectra of **3d** (1.00×10^{-4} M) in the presence of **4** (1.00×10^{-2} M): 25 °C, dichloromethane:ethyl acetate = 30:1 v/v. Similar CD spectra were observed for (1R,2R)-and (1S, 2S)-**5**: the CD sign of (1R,2R)-**5** coincides with that of L-**4**

RESULTS AND DISCUSSION

Positive Homotropic Allosterism in 3d

In order to solubilize both double decker porphyrins and dicarboxylic acid guests, the spectral measurements were carried out in dichloromethane:ethyl acetate = 30:1 v/v at 25 °C. As chiral guest molecules, we chose five α-amino acid derivatives (BOC-L-aspartic acid (L-**4**), BOC-L-glutamic acid, BOC-L-serine, BOC-L-histidine, and di-BOC-L-cystine), L-tartaric acid, L-tartaric acid dimethyl ester, and (1R,2R)-cyclohexane-1,2-dicarboxylic acid ((1R,2R)-**5**).

Firstly, circular dichroism (CD) spectra of **3d** were measured in the presence of eight equivalents of guest. As shown in Figure 1, exciton-coupling-type CD bands were clearly observed for **3d** in the presence of L-**4**. Almost same bands have been observed in the presence of (1R,2R)-**5**. Compound **3d** was CD-silent in the presence of the residual six guest molecules. On the other hand, **3a'** was CD-silent in the presence of all guest molecules. The results indicate that the strong CD bands in Figure 1 can be observed only for the certain host-guest combinations. In Figure 2, the $[\theta]_{max}$ at 310 nm is plotted against the guest concentration. It can be seen clearly from Figure 2 that the plots feature sigmoidal curvature, indicating that the guest-binding to **3d** occurs cooperatively. This cooperative guest-binding process can be analyzed according to the Hill equation[19]: $\log(y/(1-y)) = n\log[\text{guest}] + \log K$, where K and n are the association constant and Hill coefficient, respectively and $y = K/([\text{guest}]^{-n} + K)$. From the slope and the intercept of the linear plots we obtained $K = 2.63\times10^{11}$ M^{-4} and $n = 3.9$ for L-**4** (correlative coefficient 0.988) and $K = 2.75\times10^{9}$ M^{-4} and $n = 4.0$ for (1R,2R)-**5**(correlative coefficient 0.995). The 1:4 stoichiometry of the CD-active species was further corroborated by a Job plot.[20] As shown in Figure 3, a plot of $[\theta]_{max}$ at 310 nm against [**3d**]/([**3d**] + [L-**4**]) results in a maximum at 0.2, which supports the view that the complex consists of one **3d** host and four L-**4** guests. The foregoing findings consistently indicate that four pairs of 4-pyridyl groups in **3d** cooperatively bind these chiral guest molecules and that the two porphyrin planes are immobilized asymmetrically by the formation of bridge-type hydrogen bonds with chiral dicarboxylic acids to yield CD-active species: hence, this is a rare artificial system for which a sharp positive allosterism with $n = 4$ is observable. The facts that the particularly strong CD bands appear when chiral guests form cyclic host·guest complexes and the stoichiometry between **3d** host and dicarboxylic acid guests is 1:4 (but not 1:8) also support the formation of the four bridge-type hydrogen bonds.

^{1}H NMR Spectra of 3d and 3a'

Here, two essential questions come to our mind: they are (1) why **3d** can bind the dicarboxylic acid guests whereas **3a'** cannot and (2) why only **4** and **5** result in a CD-active species with **3d**. To solve the first question we measured the ^{1}H NMR spectra of L-**4** in the presence of **3d** (1.00×10^{-3} M) (25 °C, CD_2Cl_2:$CD_3COC_2D_5$ = 30:1 v/v). The chemical shifts of NH, α-CH, and β-CH_2 protons in L-**4** moved to lower magnetic field (from 5.59 to 5.70 ppm for NH, from 4.56 to 4.62 ppm for α-CH, and from 2.95 to 3.06 ppm for β-CH_2 owing to the anisotropic effect of the **3d** porphyrin rings and the plots of Δδ versus [L-**4**] showed sigmoidal curvatures similar to those in Figure 2. In contrast, **3a'**cannot induce such a downfield shift at all for these protons in L-**4**; the difference clearly discloses the mechanistic origin of the present positive homostopic allosterism. Host **3a'** bearing only one pair of pyridyl groups should have a potential to bind **4** or **5** through a hydrogen-bonding interaction but the absence of the chemical shift change in ^{1}H NMR spectroscopy suggests that this site does not appreciably interact with dicarboxylic acid

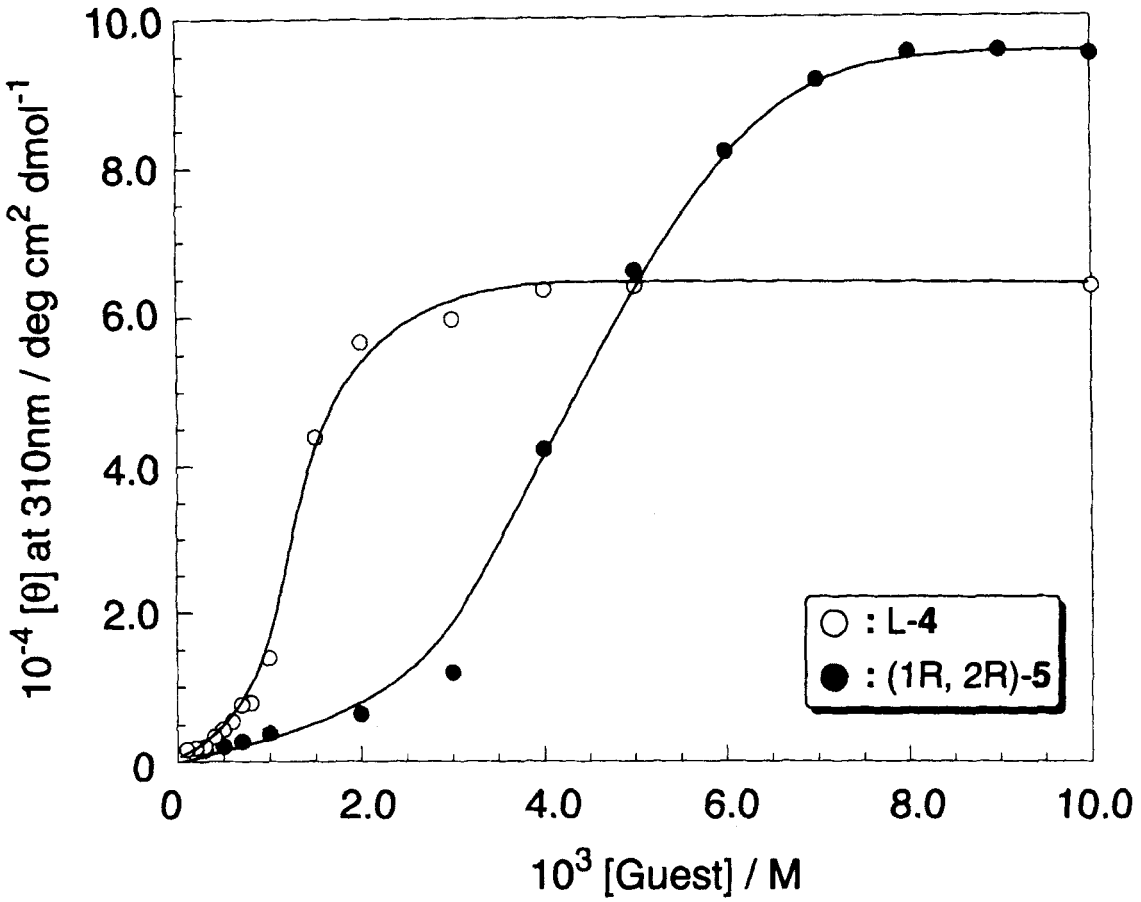

FIGURE 2 Plots of $[\theta]_{max}$ at 310 nm for **3d** versus [guest]: the measurement conditions are reported in the caption to Figure 1

guests; in other words, the association constant (K_1) for acceptance of the first guest is very small in **3a'**. Conceivably, the free energy gain obtained from the pyridine-carboxylic acid interaction is sufficiently offset by the free energy loss consumed for suppression of the porphyrin ring rotation. This is also the case in **3d** for the binding of the first guest; in **3d**, however, once the porphyrin ring rotation is suppressed by the first guest, the subsequent binding of the second, third, and fourth guests can occur successively without such a free energy loss. This means suppression of porphyrin ring rotation becomes more favorable upon succesive guest binding and so association occurs more efficiently (Figure 4). This type of guest-binding results in only the complex with 1:4 stoichiometry. As described later on the basis of comparison between **3a** and **3a'**, the pyridine-carboxylic acid interaction is somewhat intensified by electron-donating substituents introduced into the meso-phenyl groups. Since the phenyl group is more electron-donating than the 4-pyridyl group, the K_1 for **3a'** should be larger than that for **3d**, nevertheless, significant guest binding was observed for **3d** but not for **3a'**. This difference clearly demonstrates the importance of positive allosterism which can stabilize the final 1:4 complex after the cooperatively guest binding.

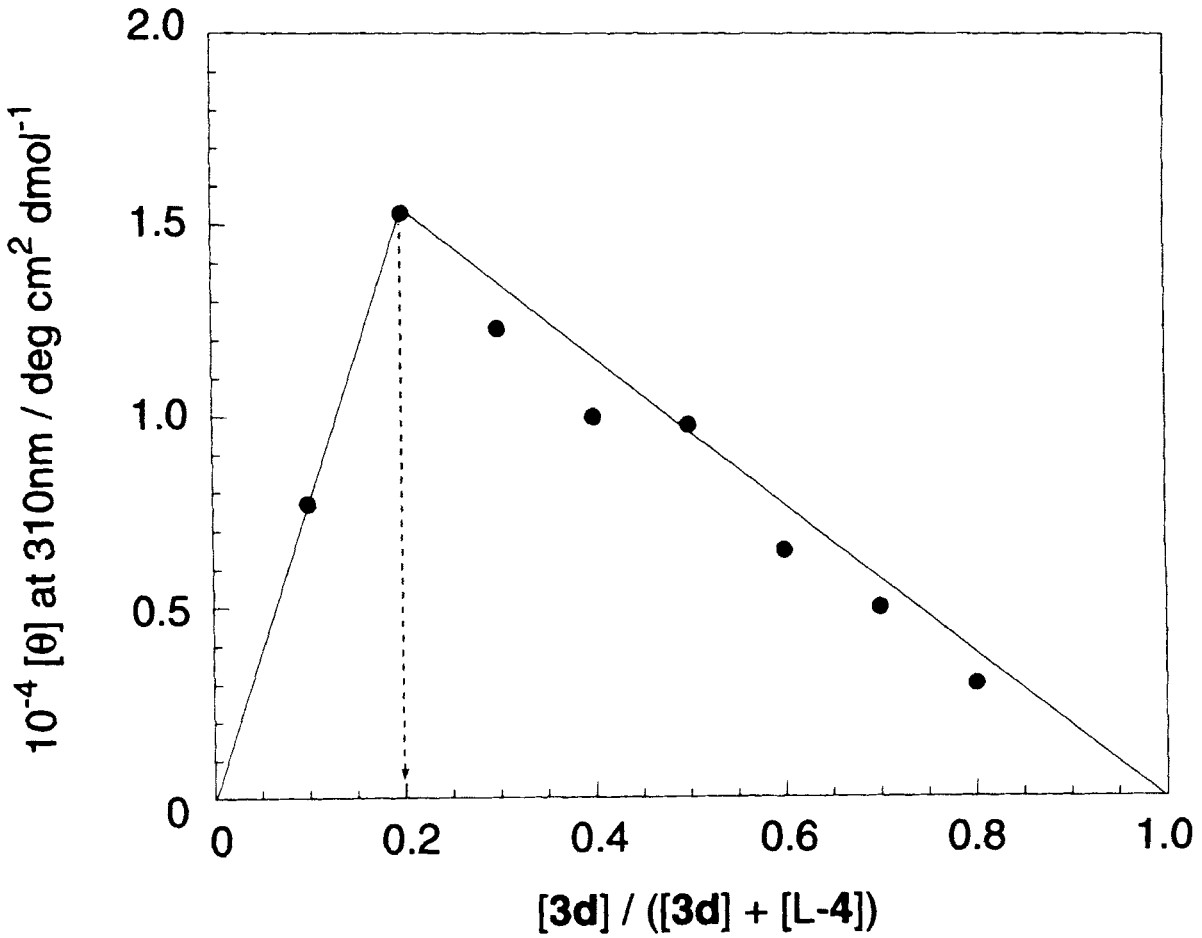

FIGURE 3 Job plot: the [**3d**] +[L-**4**] value is maintained constant (1.00×10^{-3} M)

According to X-ray crystallographic studies of cerium(IV) bis(porphyrinate) double deckers, the distance between the two porphyrin planes is about 3.4 Å.[15c] This distance is comparable with that between two carboxylic acid groups in **4** and **5** which are separated by a dimethylene spacer, and therefore, they can easily bridge two porphyrin rings. In these complexes, two porphyrin rings are twisted either in a right-handed manner or a left-handed manner, depending on the guest chirality, but the distance between the two porphyrin planes is not altered by cooperative guest-binding. BOC-L(or D)-glutamic acid with a trimethylene spacer cannot satisfy these requirements and therefore cannot result in the CD-active species. It is remarkable that a difference of one methylene unit can be precisely recognized in an all- or-nothing manner, which is due to the multiplication of a small difference through the positive allosteric binding process. On the other hand, L-tartaric acid with a dimethylene spacer satisfies the basic structural requirement as a guest molecule. When a dichloromethane solution of **3d** and an ethyl acetate solution of L-tartaric acid were mixed, a colored precipitate was formed immediately.

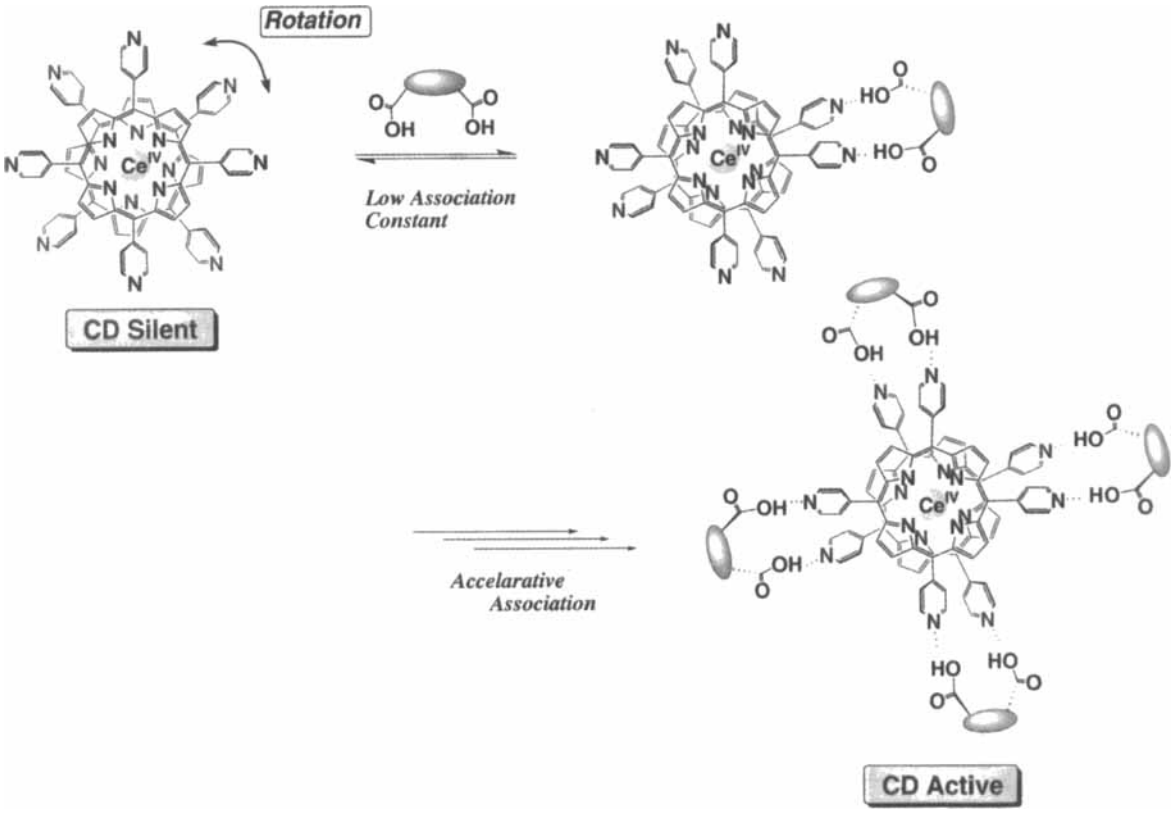

FIGURE 4 Schematic representation of the cooperative binding of **4** or **5** to **3d** (See Color Plate I at the back of this issue)

The elemental analysis of which established that it consisted of one **3d** host and four L-tartaric acid guests.[21]

Positive Homotropic Allosterism in $3b_p$, $3b_d$, and 3c

To obtain further insights into the positive homotropic allosterism we synthesized $\mathbf{3b_p}$ and $\mathbf{3b_d}$ with two pairs of 4-pyridyl groups and **3c** with three pairs of 4-pyridyl groups. Since the residual *meso*-substituents were 4-methoxyphenyl groups, we used **3a** with one pair of 4-pyridyl groups and three pairs of 4-methoxyphenyl groups as a reference compound.

As shown in Figures 5 and 6 (at [L-**4**] = [(1R,2R)-**5**] = 1.00×10^{-2} M where the CD spectral change has been saturated), **3a** gave a CD-active species with L-**4** and (1R,2R)-**5** although the CD intensity was relatively weak. This result is in contrast to that for **3a'** which could not give any CD-active species. The difference is attributed to the presence of three pairs of electron-donating 4-methoxyphenyl groups which enhance the hydrogen-bond accepting properties of the 4-pyridyl groups. The CD spectra for $\mathbf{3b_p}$, $\mathbf{3b_d}$, and **3c** were also measured in the presence of excess L-**4** and (1R,2R)-**5** where the spectral changes were saturated. The CD spectral data thus obtained are summarized in Table I. It can be seen from Figures 5 and 6 that the CD intensity at around 310 nm (π-π^* transition band of the 4-pyridyl moiety) increases with the increase in the number of the 4-pyridyl groups.

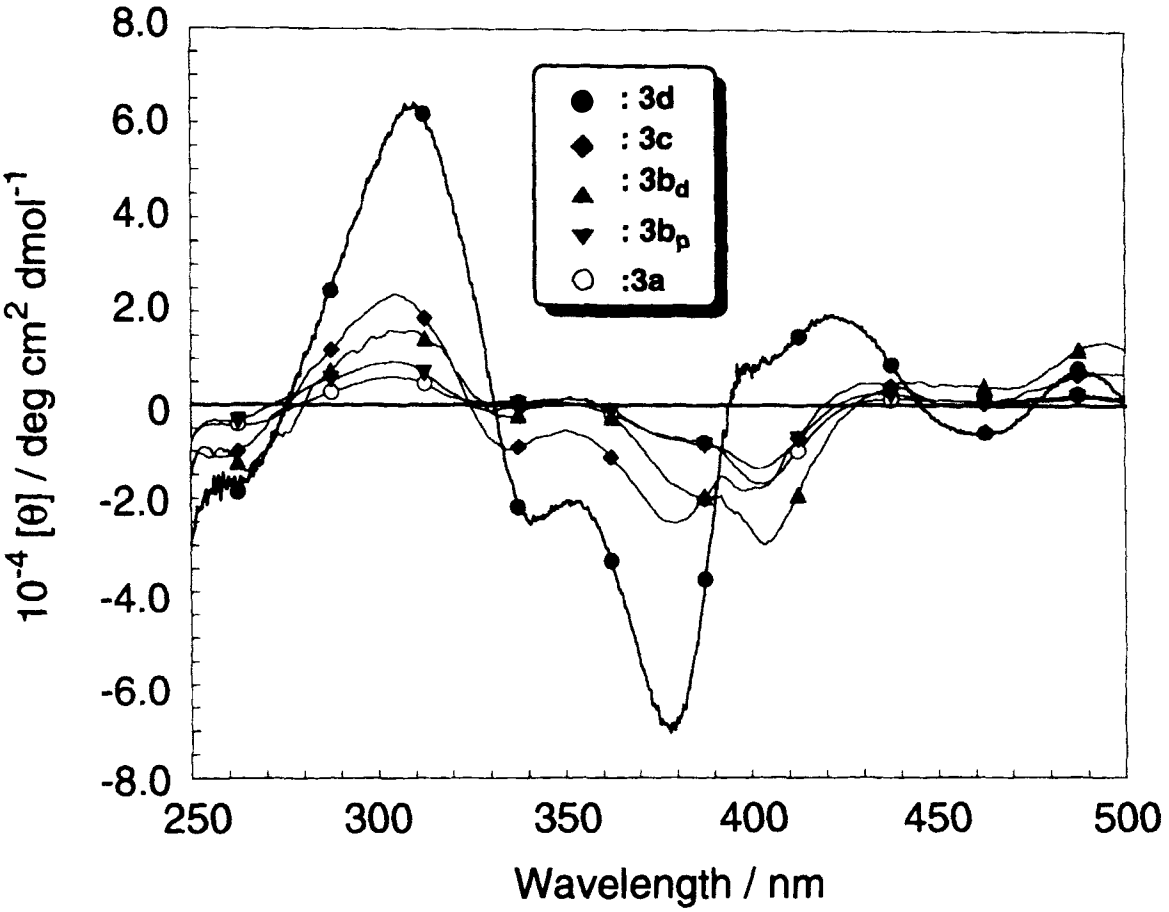

FIGURE 5 CD spectra of **3a**, **3b$_p$**, **3d$_d$**, **3c**, and **3d** (1.00×10^{-4} M) in the presence of L-**4** (1.00×10^{-2} M)

This implies that this band is related to induced CD (ICD) arising from the interaction between the 4-pyridyl groups and chiral dicarboxylic acid guests. In fact, plots of the θ against the number of 4-pyridyl pairs show a good linear relationship.

The stoichiometry for these complexes was estimated by a Job plot[19] between the θ (at 305 nm) and [double decker]/([double decker] + [(1R,2R)-**5**]). As shown in Figure 7, **3a**, **3b$_p$** and **3b$_d$** give a maximum at 0.50 and 0.33, respectively, indicating that these compounds form 1:1 complex in the case of **3a** and 1:2 complexes in the case of **3b$_p$** and **3b$_d$**. On the other hand, it was difficult to estimate the stoichiometry for the complex with **3c** because it did not show the sufficient solubility in a mixed solvent of dichlomethane: ethyl acetate (30:1 v/v). Since the θ *vs.* [double decker] plots for **3b$_p$**, **3b$_d$**, and **3c** showed sigmoidal curves similar to those for **3d** (Figure 8), they were "tentatively" analyzed by Hill equation.[19] On the other hand, the plot for **3a** was analyzed according to conventional Benesi-Hildebrand equation[22] assuming the formation of a 1:1 complex. The results are summarized in Table II.

TABLE I CD parameters of hydrogen-bonding complexes of **3** to (1R,2R)-**5**[a]

	λ_{max} or λ_{min} ($10^{-4}[\theta]_{obs}$ / deg $cm^{-2}dmol^{-1}$)		
	260.0(-1.4)	305.0(2.1)	
			341.0(0.54)
3a	380.0(-2.0)	401.0(-4.2)	
			438.0(0.63)
	490.0(1.8)		
	260.0(-2.3)	305.0(3.3)	330.0(-2.9)
$\mathbf{3b_p}$	349.0(0.32)	380.0(-2.8)	402.0(-4.4)
	435.0(0.65)	491.5(0.84)	
	265.5(-3.9)	305.0(4.4)	330.0(-2.9)
$\mathbf{3b_d}$	349.0(0.32)	380.0(-2.8)	402.0(-4.4)
	435.0(0.65)	491.5(0.84)	
	257.0(-2.6)	305.0(6.3)	
3c	379.0(-5.4)	401.0(-3.2)	334.5(-1.6)
			431.5(1.7)
	491.0(2.3)		
	251.0(5.1)	310.0(8.1)	340.0(-2.0)
3d	350.0(-1.9)	382.0(-7.8)	402.0(0.45)
	408.0(0.18)	440.0(2.3)	495.0(5.2)

[a] 25°C, dicholoromethane:ethyl acetate = 30:1 v/v, **3** (1.00×10^{-4} M) in the presence of (1R,2R)-**5** (1.00×10^{-2} M)

TABLE II Binding parameters obtained from Hill's plot and B-H plot

Host	*log K*	n_H	*Stoichiometry*[a]	*R*
3a	2.3[b]	1.0	1:1	0.96
$\mathbf{3b_p}$	4.4	1.5	1:2	1.00
$\mathbf{3b_d}$	4.7	1.7	1:2	1.00
3c	8.4	3.0	nd	0.98
3d	9.4	4.0	1:4	0.98

a. From Job plot.
b. From B-H plot.

Examination of Table II reveals that **3c** gives $n = 3.0$ supporting the view that the complex consists of 1:3 **3c**/(1R,2R)-**5** and the complexation occurs according to positive homotropic allosterism. Hence, one can regard that the K_1 for the binding of the first guest is much smaller than the K_2 and K_3 for the binding of the second and third guests. In contrast, the plots for $\mathbf{3b_p}$ and $\mathbf{3b_d}$ give $n = 1.5$ and 1.7, respectively, which are significantly smaller than 2.0. These results suggest that in $\mathbf{3b_p}$ and $\mathbf{3b_d}$ K_1 is not sufficiently smaller than K_2. Hence, the plots were analyzed by a non-linear least-squares method assuming two-step binding with K_1 and K_2. The K_1 and K_2 values for $\mathbf{3b_p}$ were 610 M^{-1} and 750 M^{-1}, respectively, whilst those for $\mathbf{3b_d}$ were 400 M^{-1} and 930 M^{-1}. What is the origin of the difference in K_1 and K_2 between $\mathbf{3b_p}$ and $\mathbf{3b_d}$? In the more symmetrical $\mathbf{3b_d}$, two pairs of adjacent 4-pyridyl groups which are useful for the guest binding are always provided regardless of the porphyrin

ring rotation (Figure 9A). In the less symmetrical $\mathbf{3b_p}$, on the other hand, porphyrin ring rotation allows not only a conformer bearing two pairs of adjacent 4-pyridyl groups but also another conformer bearing only one pair of adjacent 4-pyridyl groups (Figure 9B). This conformational difference explains that K_2/K_1 (= 2.3) and n (= 1.7) for more symmetrical $\mathbf{3b_d}$ are greater than those for less symmetrical $\mathbf{3b_p}$(K_2/K_1 = 1.2 and n= 1.5, respectively). However, it is difficult to explain why the K_1 (= 400 M^{-1}) for $\mathbf{3b_d}$ is somewhat smaller than that (= 610 M^{-1}) for $\mathbf{3b_p}$. In $\mathbf{3b_d}$ the electron-donating 4-methoxyphenyl groups occupy the *trans*-position to the 4-pyridyl groups whereas in $\mathbf{3b_p}$ they occupy the *cis*-position and the electron-withdrawing 4-pyridyl groups occupy the *trans*-position. Provided that the resonance effect arising from the *trans*-position is more influential than that from the *cis*-position, it is reasonable that the 4-pyridyl groups in $\mathbf{3b_p}$ possess the higher ability as a hydrogen-bond acceptor. The enantiomeric relationship between rotational isomers linked by horizontal arrows in Figure 9 may also play a role in discriminating between chiral guests but the diastereomeric relationship between the vertically linked rotational isomers of $\mathbf{3b_p}$ is probably the most important here.

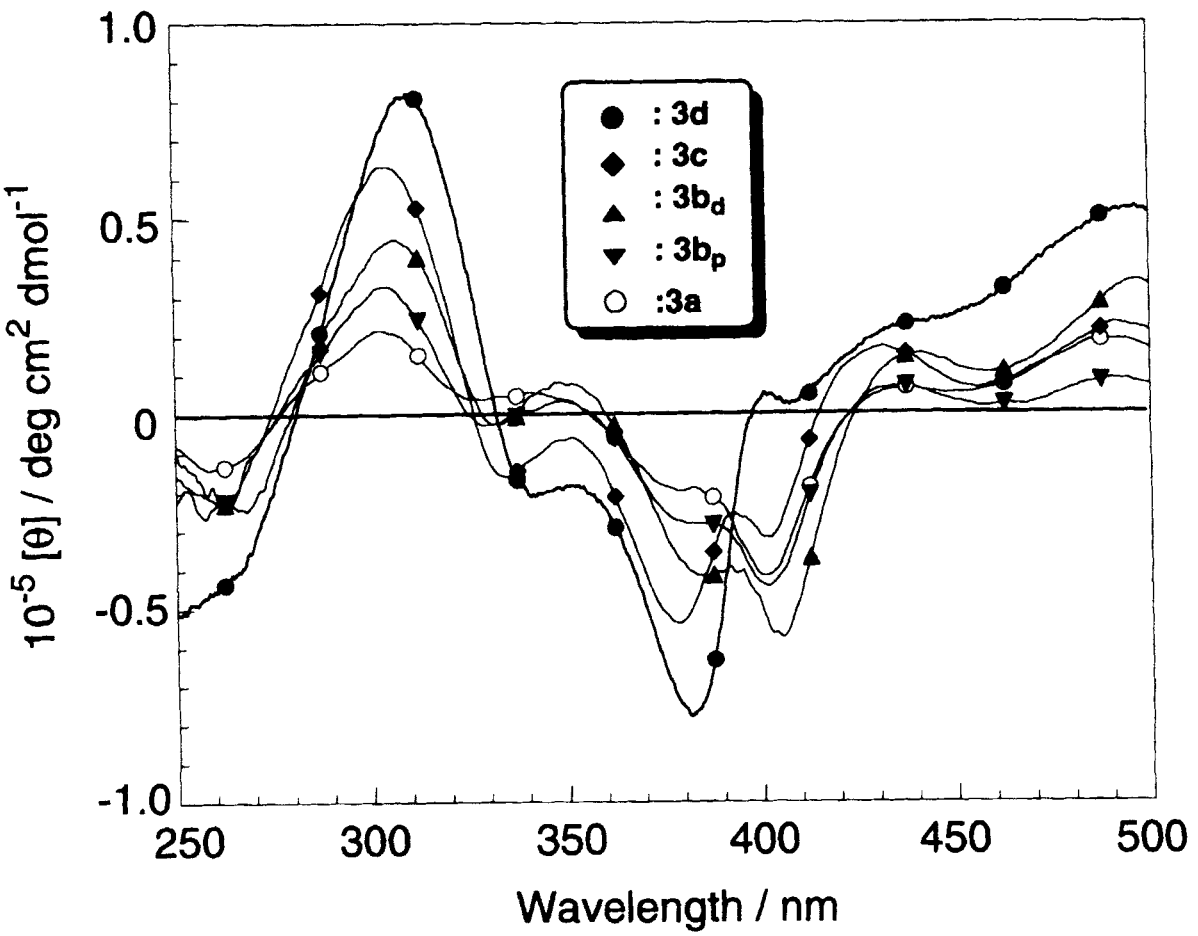

FIGURE 6 CD spectra of **3a**, $\mathbf{3b_p}$, $\mathbf{3b_d}$, **3c**, and **3d** (1.00×10^{-4} M) in the presence of (1R,2R)-**5**(1.00×10^{-2} M)

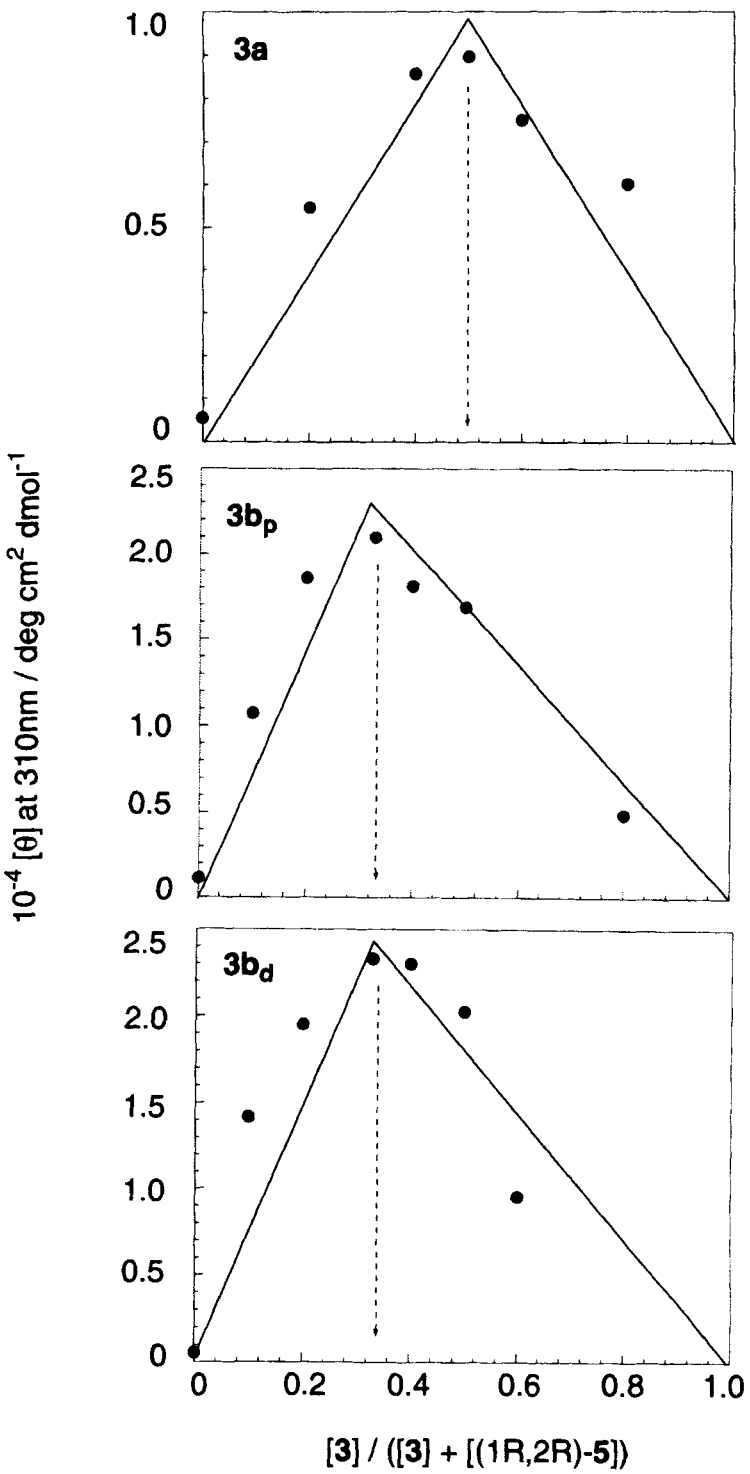

FIGURE 7 Job plots: the [3] + [(1R,2R)-5] values are maintained constant (1.00×10^{-3} M)

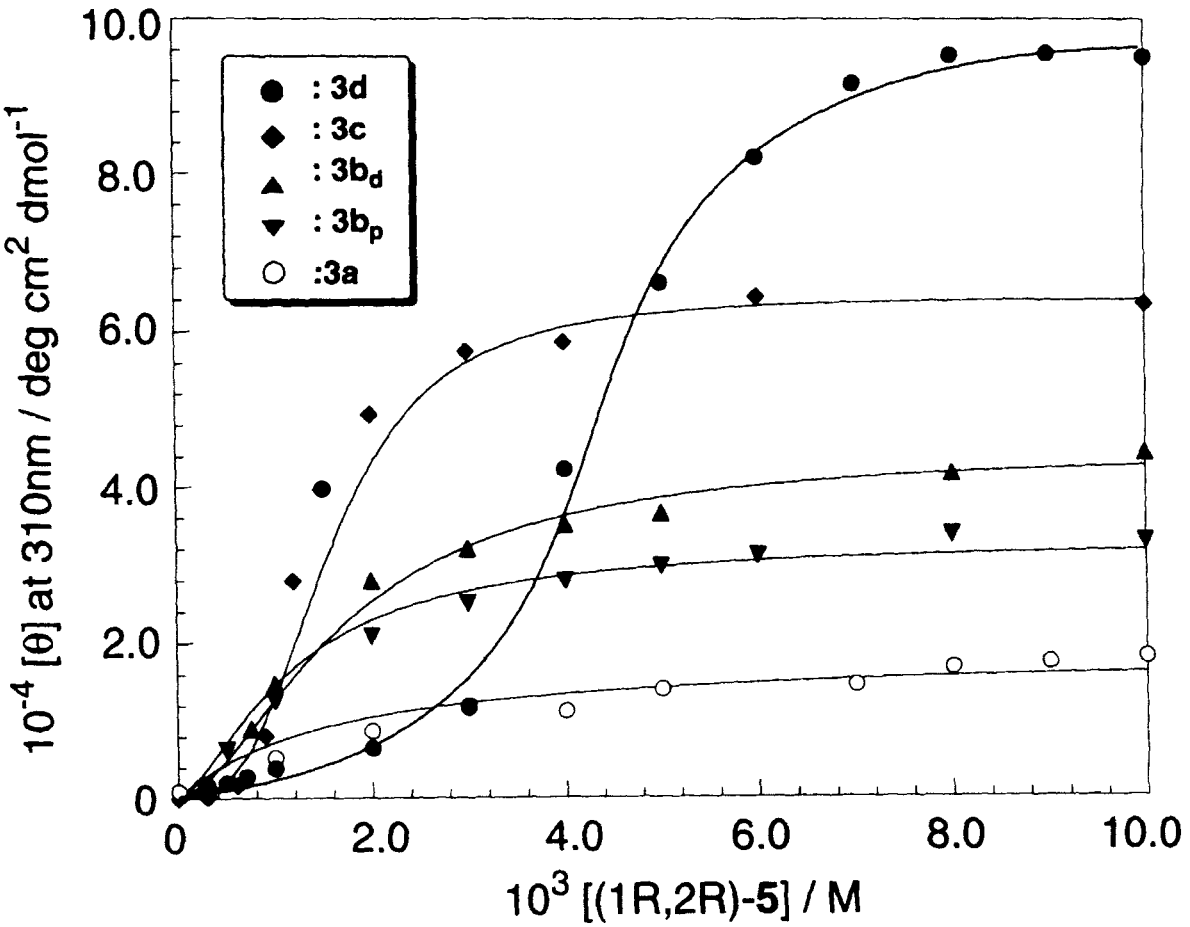

FIGURE 8 Plots of $[\theta]_{max}$ at 310 nm for **3a**, **3b$_p$**, **3b$_d$**, **3c**, and **3d** versus [(1R,2R)-5]

^{1}H NMR Spectra of 3c

To obtain further insights into allosteric guest binding modes we measured ^{1}H NMR spectra in dichloromethane-d_2: ethyl-d_5 acetate-d_3 = 30:1 v/v. For this purpose we used (1R,2R)-**5** as a guest which is more symmetrical than L-**4** and expected to give the simpler ^{1}H NMR spectra. As mentioned above, the down-field shift of the guest proton peaks was also observed for (1R,2R)-**5**. In contrast, those of cerium(IV) double decker porphyrins were significantly broadened at room temperature and any significant information could not be obtained. We thus lowered the temperature of the sample solutions to −20 °C, where those of **3b$_p$**, **3b$_d$**, and **3d** resulted in the precipitate. Very fortunately, the solution of **3c** was still homogeneous. We thus collected the ^{1}H NMR data using this sample solution.

In the absence of guests, the ^{1}H NMR peaks are sharpened with lowering temperature (Figure 10a). At −20 °C it becomes clear that these sharpened peaks are assignable to 4-meth-

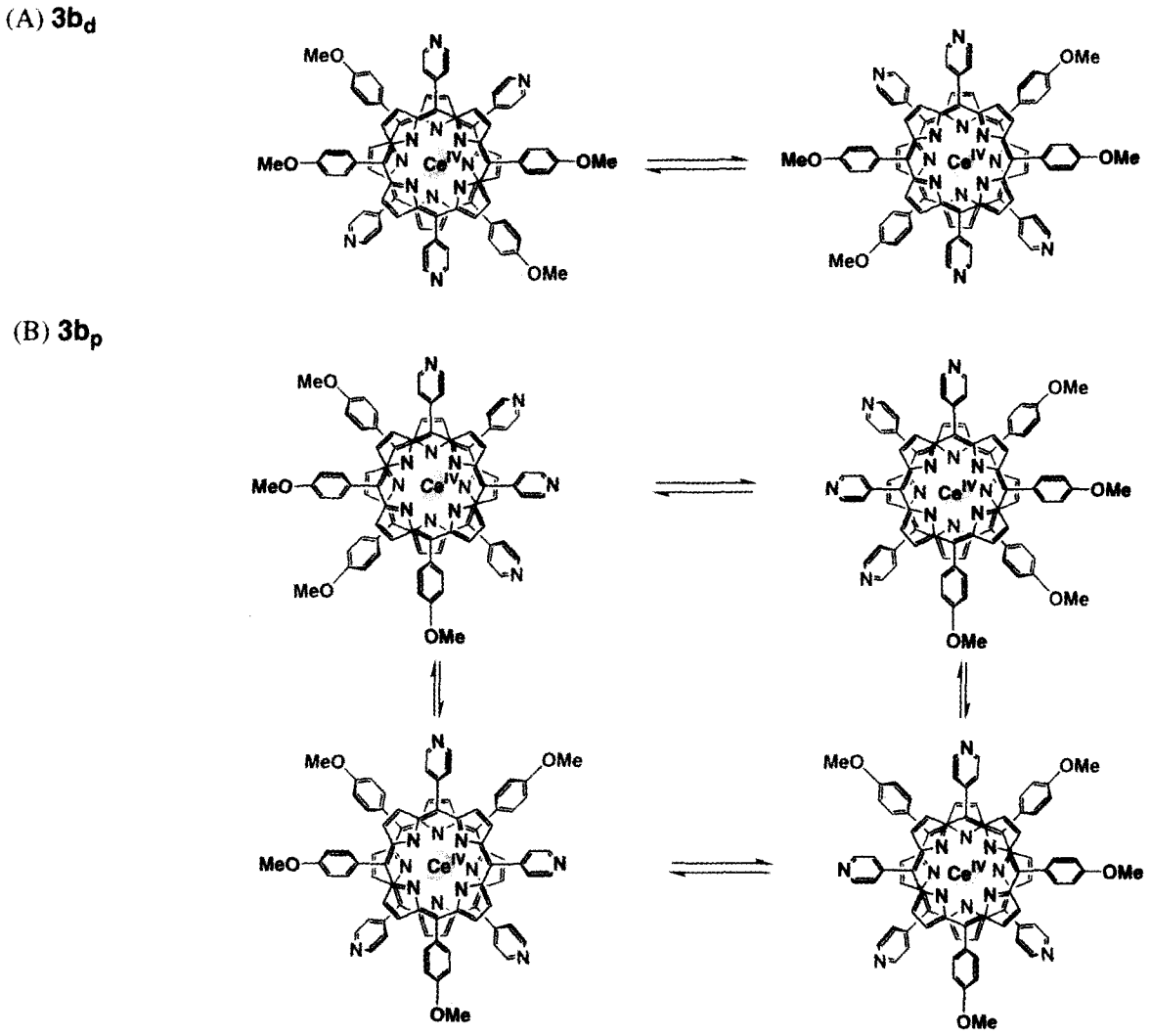

FIGURE 9 Conformational isomerism induced by the porphyrin ring rotation: (A) $\mathbf{3b}_d$ and (B) $\mathbf{3b}_p$ (See Color Plate II at the back of this issue)

oxyphenyl and 4-pyridyl protons. This implies that these aryl groups are rotating in a speed comparable with the NMR time-scale and the coalescence temperatures exist at around 25 °C. On the other hand, the peak width of the pyrrole protons is scarcely affected, indicating that the rotation speed of the porphyrin planes is much slower than the NMR time-scale.[16,17] It is seen from Figure 10 that most aryl peaks move to lower magnetic field upon complexation with (1R,2R)-**5** (Figure 10b). In particular, most of the aryl protons in the 4-pyridyl groups feature the large down-field shift, whereas those in the 4-methoxyphenyl groups are much less affected. The result indicates that carboxylic acid protons form the hydrogen bonds with the pyridine nitrogens. It is also seen from Figure 10 that at 25 °C the peaks (particularly, those of the 4-pyri-

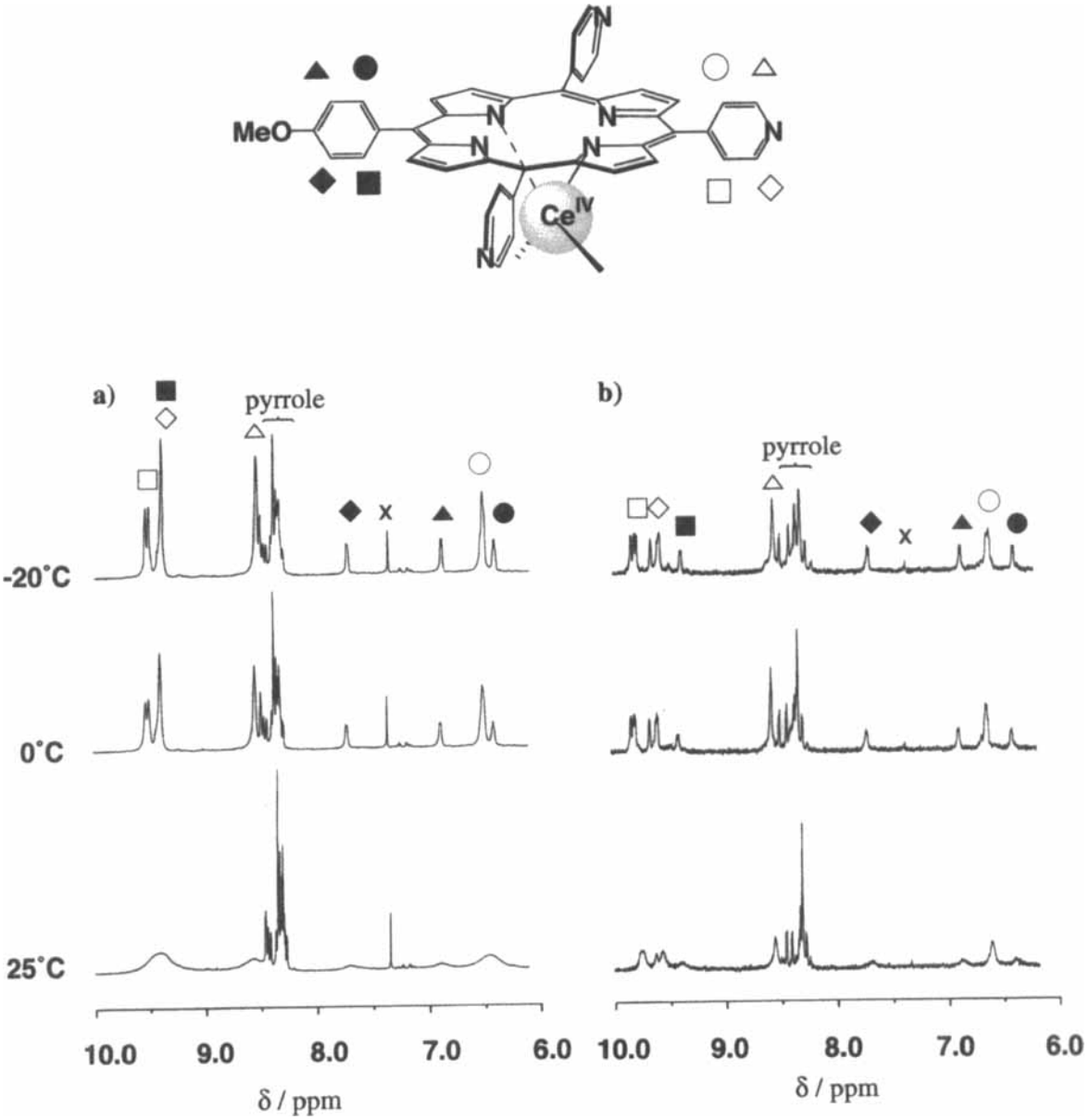

FIGURE 10 ^{1}H NMR spectra of **3c** (0.50×10^{-3} M: 600 MHz, dichloromethane-d_2:ethyl-d_5 acetate-d_3 = 30:1 v/v) in the absence and the presence of (1R,2R)-**5** (1.50×10^{-3} M)

dyl groups) in the presence of (1R,2R)-**5** are sharper than those in the absence of (1R,2R)-**5**. This suggests that the coalescence temperature becomes higher by guest complexation: *i.e.*, the hydrogen-bonding interaction suppresses the rotation of the 4-pyridyl groups.

Figure 11 is an enlarged ^{1}H NMR spectrum for the *endo*-protons of the 4-pyridyl groups in

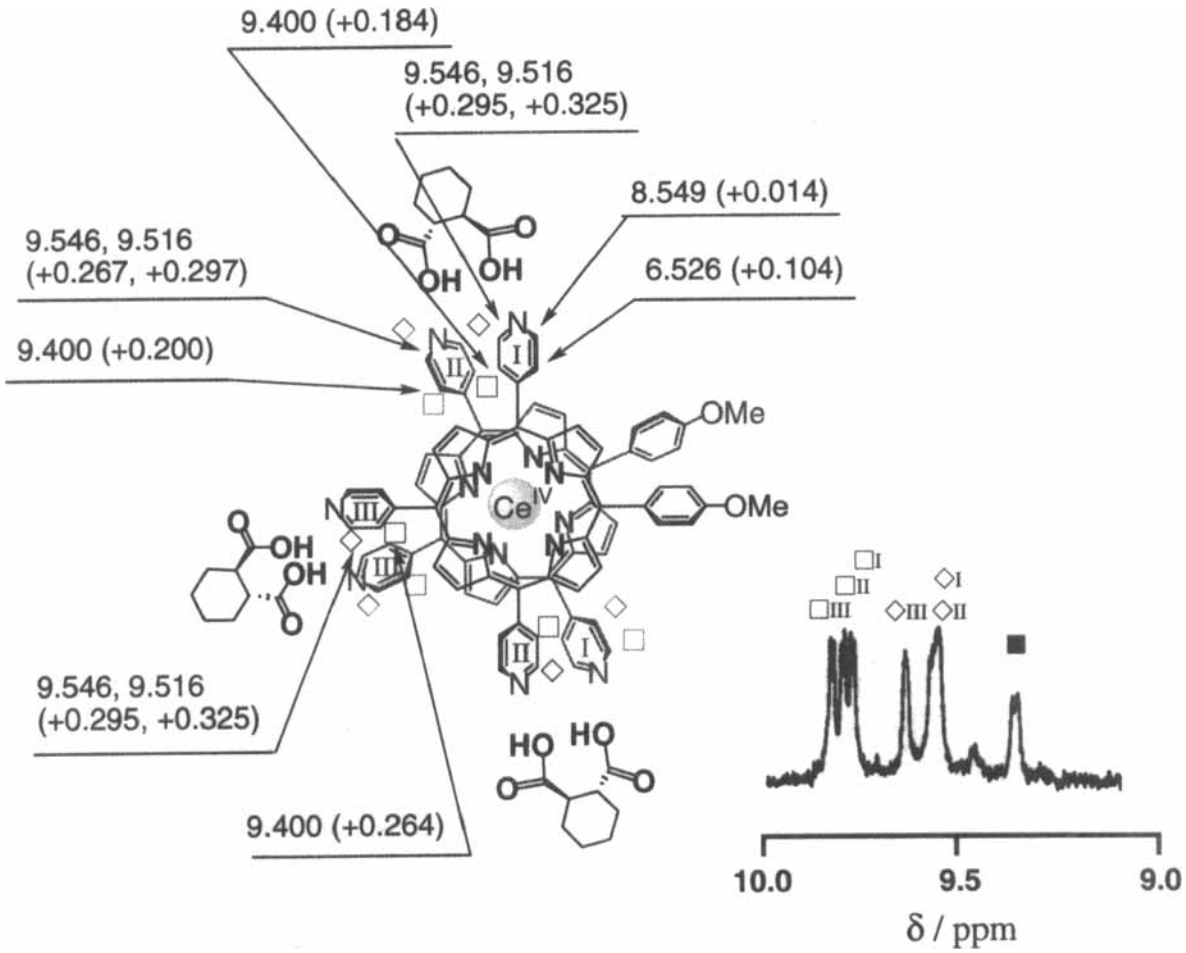

FIGURE 11 Enlarged ^{1}H NMR spectrum for the *endo*-protons of the 4-pyridyl groups in **3c** and schematic representation of **3c** chirallly-twisted by three (1R,2R)-**5** guests. One of two possible directions of chiral twist is tentatively shown here. The numbers and those in parentheses indicate the chemical shifts in the absence of guests (δ, ppm) and the shifts (Δδ) from δ, respectively

3c·[(1R,2R)-**5**]$_3$ complex. In free **3c**, pyridynes I and II are equivalent whereas they are inequivalent to pyridynes III. In chirally-twisted **3c**·[(1R,2R)-**5**]$_3$ complex, on the other hand, pyridynes I and II have become inequivalent and three inequivalent 4-pyridyl groups can exist theoretically. Very interestingly, one can count three different pyridine peaks for **3c**·[(1R,2R)-**5**]$_3$ complex (Figure 11). It is obvious that the difference between I and II is induced only by the chiral twist of two porphyrin planes. The finding supports the view that chiral (1R,2R)-**5** can really change achiral **3c** into chiral **3c** by the allosteric guest binding.

Computational and X-ray Crystallographic Studies of 3d·[(1R,2R)-5]$_4$Complex

The energy-minimized structure of **3d** was obtained by computational calculations using Insight II 98/Discover 3. The resultant structure is illustrated in Figure 12. The feasibility of this

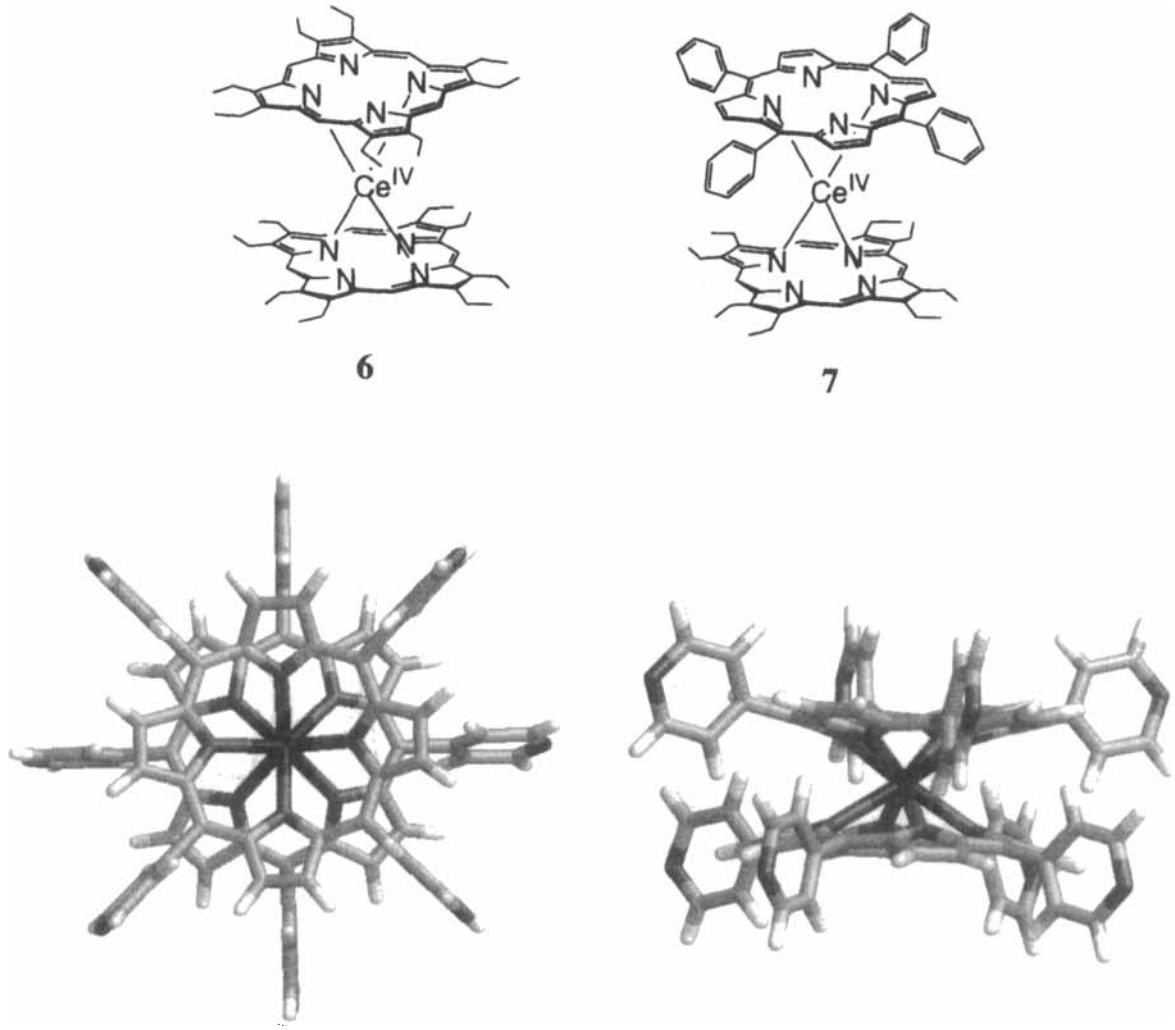

FIGURE 12 Energy-minimized structure of **3d** (See Color Plate III at the back of this issue)

structure was evaluated by comparison with X-ray structures for double decker porphyrins **6** and **7**.[15]

Firstly, the Ce-N distance is estimated to be 2.48 Å for both **6** and **7**, which shows a very good agreement with that of energy-minimized **3d** (2.49 Å: Table III). Secondly, the X-ray structures of **6** and **7**feature warped, dome-like porphyrin planes which are induced in order to relax electrostatic an and/or steric repulsion. The magnitude can be estimated by angle A which is defined as an angle between the least-squares plane of four nitrogens and that of a pyrrole ring (Figure 13). Compounds **6** and **7** have 15.5° and 13.9°, respectively[15] while energy-minimized **3d** has 18.7° (Table IV). Although angle A for energy-minimized **3d** is somewhat larger, one may consider that this is due to four bulking *meso*-4-pyridyl groups present in **3d**. Thirdly, it is known that two porphyrin planes in double decker porphyrins tend to adopt a "square antiprism" conformation in order to minimize the

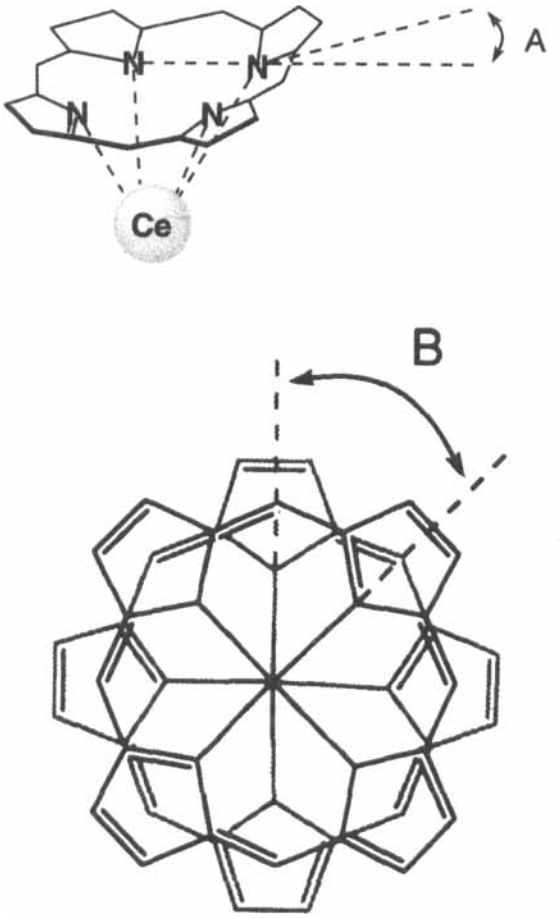

FIGURE 13 Definition of angles A and B

steric crowding. This angle (angle B as defined in Figure 13) is also similar among these three compounds: 41.8° for **6**, 44.2 ° for **7**, and 39.1° for energy-minimized **3d**. The foregoing results consistently support the view that the structure predicted for **3d** on the basis of computational calculations is very realistic.

Based on the high reliability of this computational method, we energy-minimized **3d**·[(1R,2R)-**5**]$_4$ complex according to the same method. The calculations were started from a conformation in which two carboxylic acid groups in each of four (1R,2R)-**5** molecules form two hydrogen-bonds with two 4-pyridyl nitrogens. This initial structure has angle B of 39.1°. The resultant structure is illustrated in Figure 14.

As expected, the Ce-N distance in energy-minimized **3d**·[(1R,2R)-**5**]$_4$ (2.49 Å) is scarcely changed from that in energy-minimized **3d** (2.49 Å: Table III). This is due to the rigid skeleton structure of the double decker porphyrin. Angle A in energy-minimized **3d**·[(1R,2R)-**5**]$_4$ (18.5°) is only slightly smaller than that in energy-minimized **3d** (18.7°: Table IV). This implies that two 4-pyridyl nitrogens are well preorganized so that (1R,2R)-**5** can be bound with hydrogen-bonds without a significant conformational change. On the other hand, angle B (15.8°) becomes much smaller than that before complexation (39.1°). It is clear that this angle decrease is induced by the formation of hydrogen bonds with (1R,2R)-**5**. The distances of the hydrogen bonds between pyridine N in **3d** and carboxylic acid O in (1R,2R)-**5** were estimated to be 3.39 Å and 2.80 Å. It is also worthy to mention that complexation with four (1R,2R)-**5** guests creates four deep fjords at the pyrrole bay areas. One can easily imagine that crystallization of this protuberant complex should be fairly difficult.

The single crystal of **3d**·[(1R,2R)-**5**]$_4$ complex was successfully grown up from a chloroform-ethyl acetate mixed solvent. The top view and the side view are shown in Figures 15 and 16, respectively. The unit cell structure is illustrated in Figure 17. The Ce-N distance in the crystal structure is 2.52 Å (Table V), which well coincides with those of **6**, **7**, and energy-minimized **3d**·[(1R,2R)-**5**]$_4$ (Table III). It is seen from Figure 16 that two porphyrin planes are significantly warped outward. Angle A which serves as a measure of the dome-like structure was estimated to be 13.5 °. Although this value is a little smaller than that predicted by computational calculations (18.5 °), it is very close to that for **7** (13.9 °).[15] It is likely that as predicted by the computational studies, angle A for **3d**·[(1R,2R)-**5**]$_4$ complex is larger than those for **6** and **7** because of the bulky *meso*-4-pyridyl substituents. This

TABLE III Ce - N bond lengths (Å) in **6**, (OEP) and (TPP) fragments of **7**, energy-minimized **3d** and **3d**·[(1R,2R)-5]$_4$ complex, and crystal **3d**·[(1R,2R)-5]$_4$

Bonds (Å)	6		7		Energy-minimized				Crystal
					3d		3d·[(1R,2R)-5]$_4$		3d·[(1R,2R)-5]$_4$
			OEP	TPP					
Ce – N	2.476 (3)	2.487 (3)	2.465 (3)	2.463 (3)	2.493	2.492	2.488	2.488	2.522 (4)
	2.474 (3)	2.483 (3)	2.465 (3)	2.485 (3)	2.495	2.496	2.489	2.491	
	2.467 (3)	2.474 (3)	2.481 (3)	2.475 (3)	2.493	2.495	2.484	2.487	
	2.475 (3)	2.483 (3)	2.473 (3)	2.498 (3)	2.495	2.496	2.487	2.490	
Ce – N mean values	2.475 (1)		2.471 (1)	2.480 (1)	2.494(1)		2.488(1)		2.522

TABLE IV Angle A and B (°) in **6**, (OEP) and (TPP) fragments of **7**, energy-minimized **3d** and **3d**·[(1R,2R)-5]$_4$ complex, and crystal **3d**·[(1R,2R)-5]$_4$

Angles (°)	6	7		Energy-minimized		Crystal
				3d	3d·[(1R,2R)-5]$_4$	3d·[(1R,2R)-5]$_4$
		OEP	TPP			
A mean values	15.5	13.0	14.8	18.7	18.5	13.5
B mean values	41.8	44.2		39.1	15.8	21.8

mismatch, although not so seriously different, can be rationalized as such that these bulky substituents which hamper the crystal packing are compressed in the recrystallization process. On the other hand, angle B (21.8 °) is smaller than those for **6** and **7** (41.8 ° and 44.2 ° respectively: Table IV) but somewhat larger than that for energy-minimized **3d**·[(1R,2R)-5]$_4$ (15.8 °: Table IV). From careful examination of Figure 17, we noticed that two carboxylic acid groups in (1R,2R)-**5** do not form two hydrogen bonds with two intramolecular 4-pyridyl nitrogens but with two intermolecular 4-pyridyl nitrogens. As mentioned above, **3d**·[(1R,2R)-5]$_4$ complex features a protuberant structure unfavorable to the crystal packing. Furthermore, both **3d** and (1R,2R)-**5** are rigid molecules. Hence, one may regard that one of the two hydrogen bonds is cleaved during the crystal packing process. It is undoubted, however, that the recrystallization

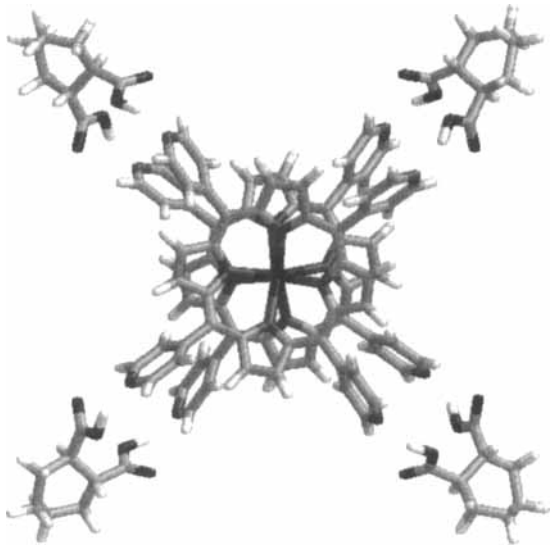

FIGURE 14 Energy-minimized structure of **3d**·[(1R,2R)-**5**]$_4$ complex (See Color Plate IV at the back of this issue)

process is still affected by the chiral guest (1R,2R)-**5**, because (i) angle B (21.8 °) is much smaller than those of **6**, **7**, and energy-minimized **3d** (*ca.* 40 °) which are not affected by a host-guest-type interaction and more or less close to angle B of energy-minimized **3d**·[(1R,2R)-**5**]$_4$ (15.8 °) and (ii) two porphyrin planes are chirally twisted with upper "right" 4-pyridyl groups and lower "left" 4-pyridyl groups in the top view (Figure 15).

CONCLUSIONS

In conclusion, we have demonstrated that the cerium(IV) double decker porphyrins show a highly positive allosteric effect through the hydrogen-bonding interaction between 4-pyridyl pairs and dicarboxylic acids. Such strong allosteric effects are very rare in artificial systems.[13] The origin of the cooperative guest binding is attributable to the successive suppression of the rotation of the porphyrin rings without deformation of the basic structure of the cerium double decker. In this context, cerium(IV) double decker porphyrins can serve as an excellent scaffold for the design of such positive allosteric systems. Thus, the present system should be readily applicable to the regulation of association processes and catalytic activities: for example, they should be useful for the efficient release or capture of dicarboxylic acid guests in solution, and hence, the catalytic activities of the porphyrins can be regulated by these guests.

EXPERIMENTAL SECTION

General

^{1}H NMR spectra were recorded either on a Brucker AC 250P(250 MHz) or Brucker DRX 600 (600 MHz) spectrometer. Chemical shifts are reported in ppm downfield from tetramethylsilane as an internal standard. Mass spectral data were obtained using either a Perseptive Voyager RP MALDI TOF mass spectrometer or JOEL JMS HX110A high-resolution magnetic sector FAB mass spectrometer. UV/vis spectra were recorded with a Shimadzu UV 160A spectrophotometer. CD spectra were recorded with a JASCO J-720WI CD spectrometer.

Syntheses of Free Base Porphyrins (H_2**3**)

Free base porphyrins were synthesized according to the method reported by Adler and Longo.[23] Hence, we here record only their analytical data.

5,15,20-Tris(4-methoxyphenyl)-20-(4-pyridyl) porphyrin (H_2**3a**)

Yield 1.02 g (3 %); ^{1}H NMR (27 °C, $CDCl_3$, 250 MHz) δ –2.11 (2H, s, NH), 4.10 (9H, s, – OCH_3), 7.31 (6H, d, J = 8.6 Hz, *m*-H in -C_6H_4-OCH_3), 8.12 (6H, d, J = 8.6 Hz, *o*-H in -C_6H_4-OCH_3), 8.15 (2H, d, J = 5.6Hz, *m*-H in -C_6H_4N), 8.88 (8H, m, pyrrole-H), 9.01 (2H, d, J = 5.7Hz, *o*-H in -C_6H_4N); MALDI TOF MS (CHCA) *m/z* 706.9 (M^+ + H, requires 706.2).

TABLE V Mean values of selected bond lengths (Å), bond angles (°), and individual values of the Ce – N bond distances with their standard deviations of **3d**·[(1R,2R)-5]$_4$

Bonds	*Lengths*[a]	*Bonds*	*Lengths*[a]
Ce – N	2.517	$C_\alpha - C_\beta$	1.36
$N - C_\alpha$	1.391 (5)	$C_\alpha - C_m$	1.404
$C_\alpha - C_\beta$	1.429 (1)		
Bonds	*Angles*	*Bonds*	*Angles*
$C_\alpha - N - C_\alpha$	105.4	$C_\beta - C_\alpha - C_m$	124.9 (6)
$N - C_\alpha - C_\beta$	110.0 (4)	$C_{py} - C_{py} - C_{py}$	119 (1)
$C_\alpha - C_\beta - C_\beta$	107.3 (9)	$C_{py} - C_{py} - N_{py}$	123.7 (9)
$C_\alpha - C_m - C_\alpha$	127.2	$C_{py} - N_{py} - C_{py}$	125.8
$N - C_\alpha - C_m$	124.9 (9)		

C_α, C_β, $C_m$denote the α and β carbon atoms of the pyrrole ring, the methine carbon atom, respectivily.
Cpy is an adjacent pyridyl carbon.

5,10-Bis(4-methoxyphenyl)-15,20-di(4-pyridyl)porphyrin (H_2**3b$_p$**)

Yield 1.80 g (6 %); ^{1}H NMR (27 °C, $CDCl_3$, 250 MHz) δ –2.82 (2H, s, NH), 4.10 (6H, s, – OCH_3), 7.31 (4H, d, J = 8.5 Hz, *m*-H in -C_6H_4-OCH_3), 8.12 (4H, d, J = 8.5 Hz, *o*-H in -C_6H_4-OCH_3), 8.16 (4H, d, J = 5.8Hz, *m*-H in -C_6H_4N), 8.79 (2H, d, J = 4.8 Hz, pyrrole-H), 8.83 (2H, s, pyrrole-H), 8.90 (2H, s, pyrrole-H), 8.94 (2H, d, J = 4.8 Hz, pyrrole-H), 9.05 (4H, d, J = 5.6Hz, *o*-H in -C_6H_4N); MALDI TOF MS (CHCA) *m/z* 677.2 (M^+ + H, requires 677.9).

5,15-Bis(4-methoxyphenyl)-10,20-di(4-pyridyl) porphyrin (H_2**3b$_d$**)

Yield 520 mg (2 %); ^{1}H NMR (27°C, $CDCl_3$, 250 MHz) δ –2.80 (2H, s, NH), 4.10 (6H, s – OCH_3), 7.32 (4H, d, J = 8.4 Hz, *m*-H in -C_6H_4-OCH_3), 8.13 (4H, d, J = 8.4 Hz, *o*-H in -C_6H_4-OCH_3), 8.18 (4H, d, J = 5.8Hz, *m*-H in -C_6H_4N), 8.81 (4H, d, J = 5.8Hz, pyrrole-H), 8.93 (4H, d, J = 5.8Hz, pyrrole-H), 9.05 (4H, d, J = 5.6Hz, *o*-H in -C_6H_4N); MALDI TOF MS (CHCA) *m/z* 677.2 (M^+ + H, requires 677.9).

5-(4-methoxyphenyl)-10,15,20-tri(4-pyridyl) porphyrin (H_2**3c**)

Yield 1.32 g (4 %); ^{1}H NMR (27 °C, $CDCl_3$, 250 MHz) δ –2.80 (2H, s, NH), 4.11 (3H, s, – OCH_3), 7.32 (2H, d, J = 8.1 Hz, *m*-H in -C_6H_4-OCH_3), 8.12 (2H, d, J = 8.1 Hz, *o*-H in -C_6H_4- OCH_3), 8.18 (6H, d, J = 5.6Hz, *m*-H in -C_6H_4N), 8.82, 8.85, 8.94 (8H, m, pyrrole-H), 9.07 (6H, d, J = 5.8Hz, *o*-H in -C_6H_4N); MALDI TOF MS (CHCA) *m/z* 648.7 (M^+ + H, requires 648.2).

Syntheses of Double Decker Porphyrins (3)

Double decker porphyrins (**3**) were synthesized from corresponding free base porphyrins(**$H_2$3**) according to the method reported by Buchler and Nawra.[15] Identification methods for **3a'**, **3a**, and **3d** have been reported previously.[17,18]

Bis[5,10-bis(4-methoxyphenyl)-15,20-di(4-pyridyl)porphyrinato]cerium(IV) (**3b$_p$**)

Yield 35 mg (21 %); ^{1}H NMR(-40°C, CD_2Cl_2, 600 MHz) δ 4.13 (12H, s, -OCH_3), 6.44 (4H, d, J= 3.8 Hz, exo *o*-H in -C_6H_4-OCH_3), 6.51 (4H, m, exo *o*-H in -C_6H_4N), 6.89 (4H, d, J = 3.8 Hz, exo *m*-H in -C_6H_4-OCH_3), 7.73 (4H, m, endo *m*-H in -C_6H_4-OCH_3), 8.33–8.46 (16H, m, pyrrole-H), 8.57 (4H, m, exo *m*-H in -C_6H_4N), 9.44–9.51 (8H, m, endo *m*-H in -C_6H_4N and endo *o*-H in -C_6H_4-OCH_3), 9.52 (4H, m, endo *o*-H in -C_6H_4N); FAB HRMS (NBA) *m/z* 1489.3986 (M^+ + H, $C_{88}H_{61}CeN_{12}O_4$ requires 1489.3993); UV-Vis (CH_2Cl_2) λ_{max} / nm (log ε) 322.5 (4.70), 397.5 (5.15), 540.5 (4.03).

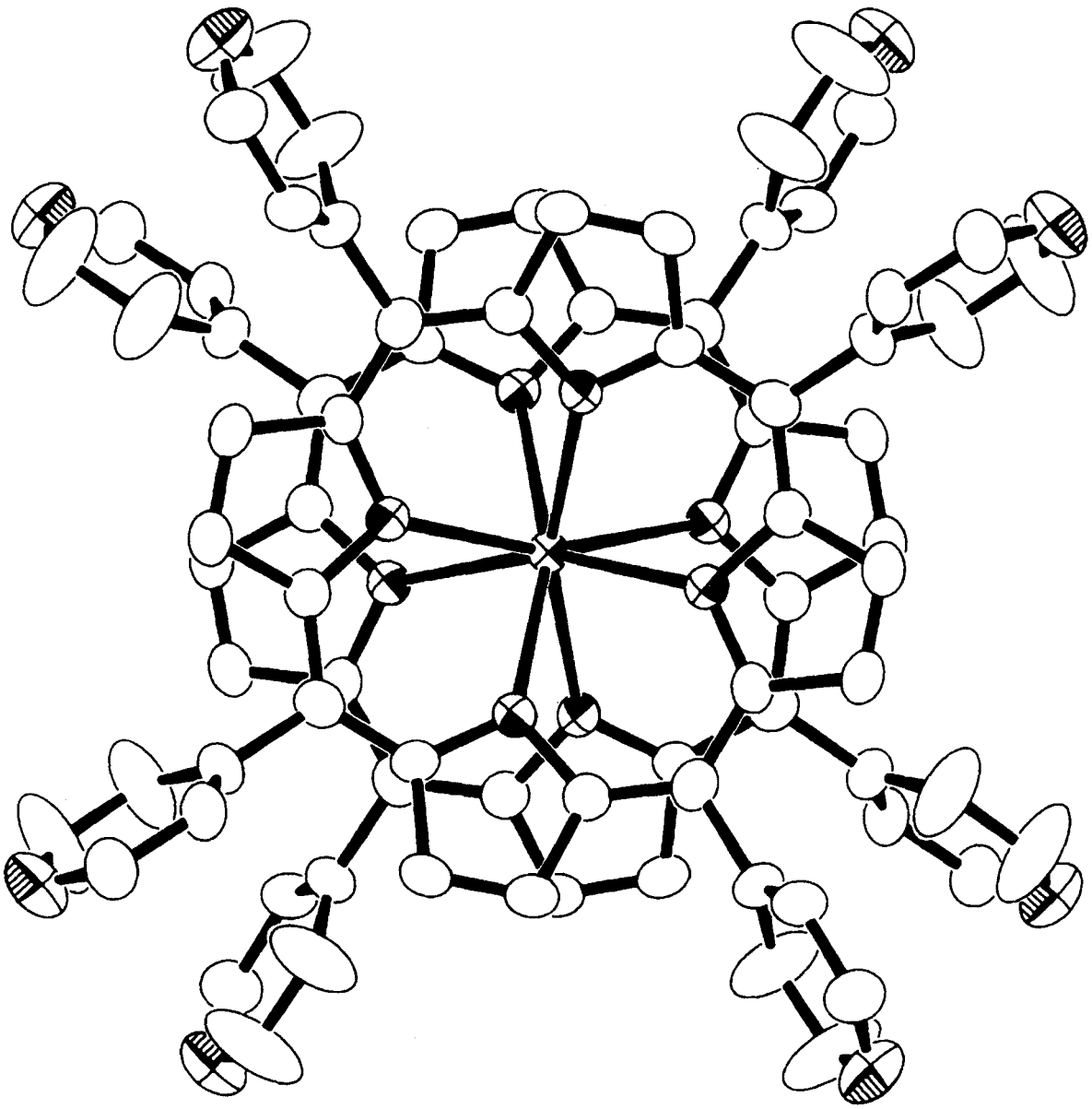

FIGURE 15 ORTEP drawing of the top view for **3d** of **3d**·[(1R,2R)-**5**]$_4$ complex. Thermal ellipsoids are drawn at the 50% level. Solvent molecules and hydrogen atoms are omitted for clarity (See Color Plate at the back of this issue)

Bis[5,15-bis(4-methoxyphenyl)-10,20-di(4-pyridyl)porphyrinato]cerium(IV) ($3b_d$)

Yield 81 mg (49 %); ^{1}H NMR(-40°C, CD_2Cl_2, 600 MHz) δ 4.13 (12H, s, -OCH_3), 6.44 (4H, d, J = 3.9Hz, exo *o*-H in -C_6H_4-OCH_3), 6.49 (4H, m, exo *o*-H in -C_6H_4N), 6.89 (4H, d, J = 3.9Hz, exo *m*-H in -C_6H_4-OCH_3), 7.73 (4H, m, endo *m*-H in -C_6H_4-OCH_3), 8.20–8.43 (16H, m, pyrrole-H), 8.57 (4H, m, exo *m*-H in -C_6H_4N), 9.43–9.46 (8H, m, endo *m*-H in -C_6H_4N and endo *o*-H in

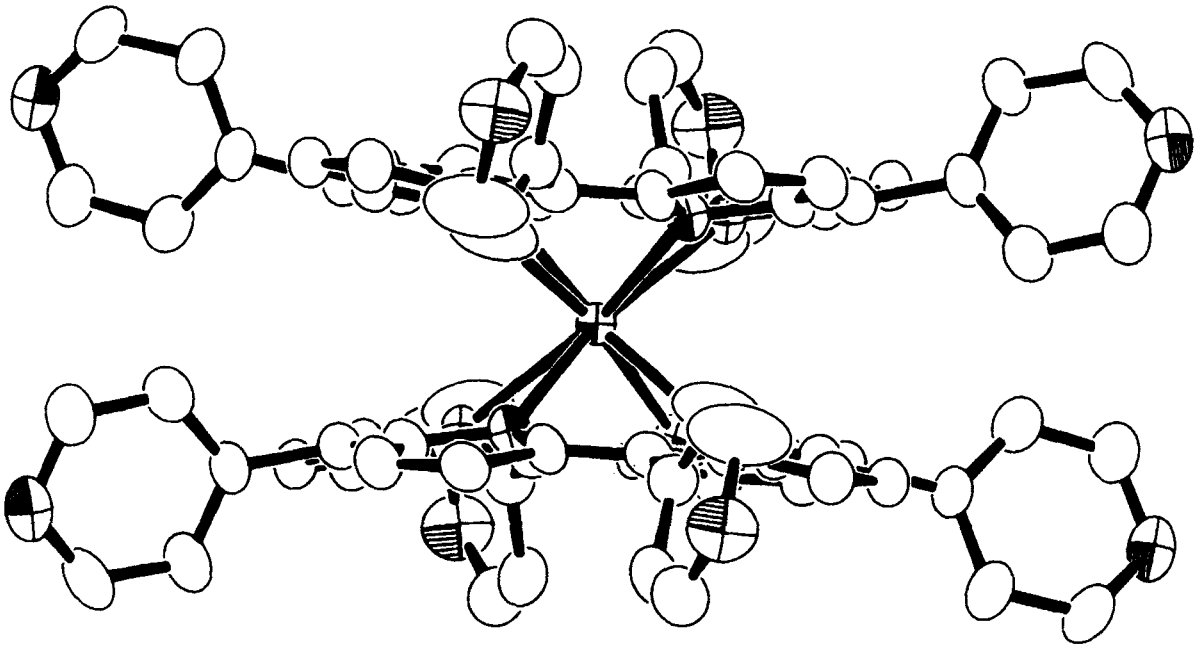

FIGURE 16 ORTEP drawing of the side view for **3d** of **3d**·[(1R,2R)-**5**]$_4$ complex

-C_6H_4-OCH_3), 9.52 (4H, m, endo *o*-H in -C_6H_4N); FAB HRMS (NBA) *m/z* 1489.3997 (M^+ + H, $C_{88}H_{61}CeN_{12}O_4$ requires 1489.3993); UV-Vis (CH_2Cl_2) λ_{max} / nm (log ε) 325.5 (4.60), 398.0 (5.21), 542.0 (3.95).

Bis[5-(4-methoxyphenyl)-10,15,20-tris(4-pyridyl)porphyrinato]cerium(IV) (3c)

Yield 34 mg (21 %); ^{1}H NMR(-40°C, CD_2Cl_2, 600 MHz) δ 4.13 (6H, s, -OCH_3), 6.43 (2H, m, exo *o*-H in -C_6H_4-OCH_3), 6.53 (6H, m, exo *o*-H in -C_6H_4N), 6.90 (2H, m, exo *m*-H in -C_6H_4-OCH_3), 7.74 (2H, m, endo *m*-H in -C_6H_4-OCH_3), 8.31–8.52 (16H, m, pyrrole-H), 8.55 (6H, m, exo *m*-H in -C_6H_4N), 9.40 (6H, m, endo *m*-H in -C_6H_4N), 9.44 (2H, m, endo *o*-H in -C_6H_4-OCH_3), 9.52 (6H, m, endo *o*-H in -C_6H_4N); FAB HRMS (NBA) *m/z* 1431.3696 (M^+ + H, $C_{84}H_{55}CeN_{14}O_2$ requires 1431.3687); UV-Vis (CH_2Cl_2) λ_{max} / nm (log ε) 322.5 (4.68), 395.0 (5.22), 540.5 (4.07).

CD Spectroscopy

To a dichloromethane solution of **3** (1.0×10^{-4}M) was injected a stock solution of dicarboxylic acid in ethyl acetate. The final solvent ratio of the measurement solution was maintained to be dichrolomethane:ethyl acetate = 30:1 (v/v). The CD spectra from 250 nm to 500 nm were recorded with a JASCO J-720WI CD spectrometer. The measurement temperature was 25 ± 0.1°C.

Crystal Data

$C_{80}H_{48}CeN_{16}$•$(C_8H_{12}O_4)_4$•$2CHCl_3$,•$4C_4H_8O_2$
M = 2648.6629, black crystal of 0.20 × 0.20 × 0.20 mm size (recrystallized from chloroform / ethyl acetate), *T* = 298 K, tetragonal, space group I422, *a* = *b* = 16.9413(4) Å, *c* = 23.6593(5) Å, *V* = 6790.5(3) Å^3, *Z* = 2, *Dc* = 1.298 g cm^{-3}, graphite-monochromated Mo-Kα radiatio, λ = 0.71069

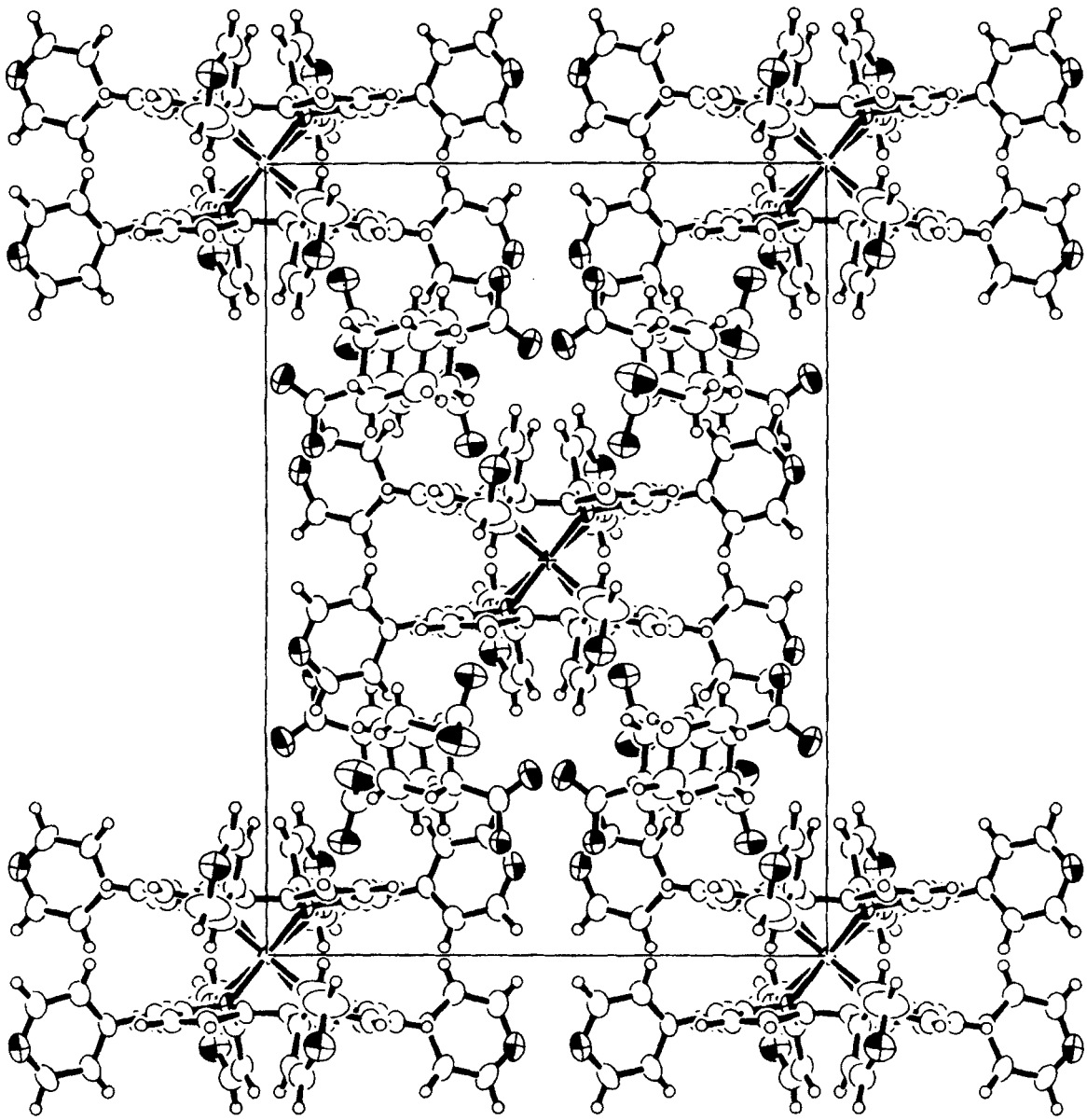

FIGURE 17 Unit cell structure for **3d**·$[(1R,2R)\text{-}5]_4$ complex

Å, $\mu = 5.25$ cm^{-1}; the data were collected on a Rigaku RAXIS imaging plate area detector diffractometer, θ-2θ scan, $2\theta < 55.0°$, 2228 reflections, 2009 observed [$I > 2.60\sigma(I)$] data. The data were corrected for Lorentz and polarization effects.

Data Collection, Structure Determination, and Refinement

The structure was solved using a direct method[24] and expanded using Fourier techniques.[25] Some non-hydrogen atoms were

refined anisotropiacally, while the rest were refined isotropically. The final cycle of full-matrix least-squares refinement was based on 2009 observed reflections [$I > 2.60\sigma(I)$] and 166 variable parameters. The final R factors were $R = \Sigma \; ||F_0| - |F_0|| \; / \; \Sigma \; |F_0| = 0.081$, $R_w = [\Sigma \; w(|F_0| - |F_c|)^2 \; / \; \Sigma \; wF_0^2]^{1/2}] = 0.111$. The standard deviation of an observation of unit weight was 1.08. The weighting scheme was based on counting statistics and included a factor (p= 0.060) to downweight the intense reflections. Plots of $\Sigma \; w(F_0^2 - F_c^2)^2$ versus, reflection order in data collection, $\sin\theta/\lambda$, and various classes of indices showed no unusual trends. The maximum and minimum peaks on the final difference Fourier map are 0.56 and –0.75 e^- / Å^3, respectively. All calculations were performed using a teXsan crystallographic software package from Molecular Structure Corporation.[26]

Computational Calculations

Calculations were performed using InsihtII 98.0 / Discover 3.00 (Molecular Simulations Inc. (MSI)) on an SGI Computer. All structures were generated using 3D Sketch and the forcefield used was ESFF. Molecular dynamics (MD) simulations were run at 500 K. The system was allowed to equilibrate for 1 ps and then MD simulations were run for 100 ps, and then minimized using the steepest descent, the conjugate gradient, and finally the Newton-Raphson methods until the first derivative of the enegy was < 0.001 kcal mol^{-1} Å^{-1}.

Acknowledgements

We thanks to Dr. Tachi for his helpful helps toward solving the X-ray structure.

References

[1] (a) Perutz, M. F. (1979). *Ann. Rev. Biochem.*, **48**, 327. (b) Monod, J., Changeux, J.-P. and Jacob, F. (1963). *J. Mol. Biol.*, **6**, 306. (c) Perutz, M. F., Fermi, G., Luisi, B., Shaanan, B. and Liddington, R. C. (1987). *Acc. Chem. Res.*, **20**, 309.

[2] Gramdori, R., Lavoie, T. A., Pflumm, M., Tian, G., Niersbach, H., Maas, W. K., Fairman, R. and Carey, J. (1995). *J. Mol. Biol.*, **254**, 150.

[3] Burke, J. R., Witmer, M. R., Tredup, J., Micanovic, R., Gregor, K. R., Lahiri, J., Tramposch, K. M. and Villaframca, J.J. (1995). *Biochemistry*, **34**, 15165.

[4] (a) Filenko, A. M., Danilova, V. M. and Sobieszek, A. (1997). *Biophys. J.*, **73**, 1593. (b) Modi, S., Gilham, D. E., Sutcliffe, M. J., Lian, L.-Y., Primrose, W. V., Wolf, C. R. and Roberts, G. C. K. (1997). *Biochemistry*, **36**, 4461. (c) Bruzzese, F. J. and Connelly, P. R. (1997). *ibid.*, **36**, 10428. (d) Schetz, J. A. and Sibley, D. R. (1997). *J. Neurochem.*, **68**, 1990.

[5] Traylor, T. G., Mitchell, M. J., Ciconene, J. P. and Nelson, S. (1982). *J. Am. Chem. Soc.*, **104**, 4986.

[6] (a) Rebek, J. Jr. (1984). *Acc. Chem. Res.*, **17**, 258. (b) Rebek, J. Jr., Costello, T., Marshall, L., Wattley, R., Gadwood, R. C. and Onan, K. (1985). *J. Am. Chem. Soc.*, **107**, 7481.

[7] (a) Tabushi, I., Kugimiya, S., Kinnaird, M. G. and Sasaki, T. (1985). *J. Am. Chem. Soc.*, **107**, 4129. (b) Tabushi, I. and Kugimiya, S. (1986). *ibid.*, **108**, 6926.

[8] Beer, P. D. and Rothin, A. S. (1988). *J. Chem. Soc., Chem. Commun.*, 52.

[9] Petter, R. C., Salek, J. S., Sikorski, C. T., Kumaravel, G. and Lin, F.-T. (1990). *J. Am. Chem. Soc.*, **112**, 3860.

[10] Schneider, H.-J. and Ref, D. (1990). *Angew. Chem. Int. Ed. Engl.*, **29**, 1159.

[11] Sijbesma, R. P. and Nolte, R. J. (1991). *J. Am. Chem. Soc.*, **113**, 6695.

[12] Kobuke, Y. and Satoh, Y. (1992). *J. Am. Chem. Soc.*, **114**, 789.

[13] (a) Kobayashi, K., Asakawa, Y., Kato, Y. and Aoyama, Y. (1992). *J. Am. Chem. Soc.*, **114**, 10307. (b) Blanc, S., Yakirevitch, P., Leize, E., Meyer, M., Libman, J., VanDorsselaer, A., Albrecht-Gray, A. M. and Shanzer, A. (1997). *J. Am. Chem. Soc.*, **119**, 4934. (c) Glass, T. E. (2000). *J. Am. Chem. Soc.*, **122**, 4522.

[14] Takeuchi, M., Imada, T. and Shinkai, S. (1996). *J. Am. Chem. Soc.*, **118**, 10658 and references cited therein.

[15] For the syntheses of metal bis(porphyrinate) double deckers see (a) Buchler, J. W. and Nawra, M. (1994). *Inorg. Chem.*, **33**, 2830. (b) Buchler, J. W., Eiermann, V., Hanssum, H.; Heinz, G., Rüterjans, H. and Schwarzkopf, M. (1994). *Chem. Ber.*, **127**, 589. (c) Buchler, J. W., De Cian, A., Fischer, J., Hammerschmitt, P., Löffler, J., Scharbert, B. and Weiss, R. (1989). *ibid.*, **122**, 2219. (d) Buchler, J. W. and Heinz, G. (1996). *ibid.*, **129**, 1073. (e) Buchler, J. W. and Heinz, G. (1996). *ibid.*, **129**, 201 and references cited therein. (f) Jiang, J., Machida, K., Yamamoto, E. and Adachi, G. (1991). *Chem. Lett.*, 2035. (g) Jiang, J., Machida, K. and Adachi, G. (1992). *Bull. Chem. Soc. Jpn.*, **65**, 1990. (h) Jiang, J., Machida, K. and Adachi, G. (1993). *J. Alloys. Comp.*, **32**, 950 and references cited therein.

[16] (a) Tashiro, K., Konishi, K. and Aida, T. (1997). *Angew. Chem. Int. Ed.*, **36**, 856. (b) Tashiro, K., Fujiwara, T., Konishi, T. and Aida, T. (1998). *Chem. Commun.*, 1121.

[17] It is known that the rate of the porphyrin ring rotation in cerium(IV) double decker porphyrins is comparable with or slower than the NMR time-scale: see Ref. (16) and Takeuchi, M., Imada, T., Ikeda, M. and Shinkai, S. (1998). *Tetrahedron Lett.*, **39**, 7897. However, allosteric behavior is observable for the present system as long as the porphyrin rings rotate.

[18] Preliminary communication: Takeuchi, M., Imada, T. and Shinkai, S. (1998). *Angew. Chem. Int. Ed.*, **37**, 2096. Application of an related system to a memory storage was recently shown: Sugasaki, A., Ikeda, M., Takeuchi, M., Robertson, A. and Shinkai, S. (1999). *J. Chem. Soc., Perkin Trans. 2*, 3259.

[19] (a) Baldwin, J. and Chothia, C. (1979). *J. Mol Biol.*, **129**, 175.
(b) Connors, K. A. (1987). *Binding Constants*, John Wiley, New York.

[20] Job, A. (1928). *Annales de Chimie (10th series)*, **9**, 113.

[21] The elemental analysis of the precipitate; Anal. Calcd for **3d**•(L-tartaric acid)$_{4.0}$: C, 58.42; H, 3.68; N, 11.35, for **3d**•(L-tartaric acid)$_{3.8}$: C, 58.83; H, 3.67; N, 11.53, for **3d**•(L-tartaric acid)$_{3.0}$: C, 60.59; H, 3.65; N, 12.29, found: C, 58.76; H, 3.68; N, 11.49. Thus, the observed result is closest to **3d**•(L-tartaric acid)$_{3.8}$. The slight deviation from the 1:4 stoichiometry is presumably due to the immediate precipitation after mixing. Although the stoichiometry in the precipitate does not always agree with that in the solution, this can be supporting evidence for the 1:4 stoichiometry.

[22] Benesi, H.A. and Hildebrand, J. H. (1949). *J. Am. Chem. Soc.*, **71**, 2703..

[23] Adler, A. D., Longo, F. R., Finarelli, J. D., Goldmachen, J., Assour, J. and Korsalioff, L. (1967). *J. Org. Chem.*, **32**, 476.

[24] SIR 97: Burla, M. C., Camalli, M., Cascarano, G., Giacovazzo, C., Polidori, G., Spagna, R. and Viterbo, D. (1989). *J. Appl. Cryst.*, **22**, 389.

[25] DIRDIF 94: The DIRDIF program system, Beurskens, P. T., Admiraal, G., Bosman, W. P., de Gelder, R., Israel, R. and Smits, J. M. M. (1994). University of Nijimegen, The Netherlands.

[26] teXsan: Crystal Structure Analysis Package, Molecular Structure Corporation (1985 and 1992).